Journal of Medicinal Chemistry

pubs.acs.org/jmc

Article

Affinity and Selectivity of Protein−Ligand Recognition: A Minor Chemical Modification Changes Carbonic Anhydrase Binding Profile

Audrius Zakšauskas, Vaida Paketurytė-Latvė, Alberta Jankūnaitė, Edita Čapkauskaitė, Yann Becart, Alexey Smirnov, Klára Pospíšilová, Janis Leitans, Jiří Brynda, Andris Kazaks, Lina Baranauskienė, Elena Manakova, Saulius Gražulis, Visvaldas Kairys, Kaspars Tars, Pavlína Řezáčová, and Daumantas Matulis*

Cite This: *J. Med. Chem.* 2025, 68, 17752−17773

Read Online

ACCESS | Metrics & More | Article Recommendations | Supporting Information

ABSTRACT: Discovery of small-molecule drugs relies on their strong binding affinity compared to nontarget proteins, thus possessing selectivity. Minor chemical structure changes usually exhibit little change in the compound efficacy, with rare exceptions. We developed a series of nearly 50 *ortho*-substituted benzenesulfonamides and experimentally measured their interactions with the 12 catalytically active human carbonic anhydrase (CA) isozymes. Inhibitors were designed using seven different substituent groups, including 4-*sulfanyl*-substituted 3-sulfamoyl benzoates and benzamides, 4-*sulfinyl*-substituted 3-sulfamoyl benzoates and benzamides, 4-*sulfonyl*-substituted 3-sulfamoyl benzoates and benzamides, and 4-amino-substituted benzamides. The oxidation state of sulfur at the *ortho* position significantly influenced the compound's affinity for CAIX, a target for anticancer drugs, demonstrating affinities hundreds of thousands of times stronger than related compounds. Coupled with X-ray crystal structures and molecular docking, the relationship between structure and thermodynamics offers insights into how small changes in the structure lead to significant changes in affinity for drug design.

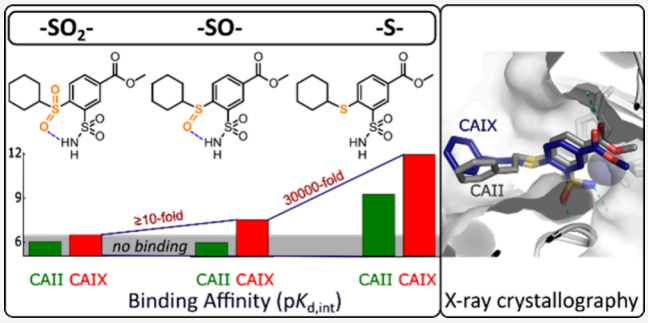

■ INTRODUCTION

A detailed understanding of protein−ligand recognition is an essential goal in small-molecule drug discovery.[1] Any drug-like chemical compound should bind the disease-related target protein with sufficiently high affinity. Furthermore, the compound must bind with high selectivity and thus not interact strongly with other nontarget proteins whose inhibition or binding could cause undesired side effects.[2] Rational design of such compounds is complex because of the limited understanding of the underlying energies of binding and how a compound recognizes and binds to the target protein.

As a model system, we study sulfonamide compound binding to human carbonic anhydrases (CA), zinc-containing enzymes.[3] Humans have 12 catalytically active CA isozymes (EC 4.2.1.1).[4−6] The enzyme catalyzes the reversible hydration of carbon dioxide and has many essential physiological functions. Since these enzymes function in pH and electrolyte homeostasis and regulation, many drugs target CA isozymes to treat diseases like glaucoma, edema, obesity, epilepsy, infertility, and cancer.[7−9] Primary sulfonamides are the most investigated CA inhibitors.[10−12] Their amino group binds directly to the catalytic zinc in the active site by forming a coordination bond and inhibits the activity of all CA isozymes. However, the binding affinity may be low or high and depends on small details of each compound arrangement on the protein surface, possible steric hindrances, or attraction due to hydrogen bonds or hydrophobic interactions.[13]

The 12 catalytically active human CA isozymes have nearly identical beta-sheet folds. Their active sites are highly similar in shape, but several amino acids in the active site vary among the isozymes.[14−16] Because the differences in the active site amino acid composition are small, it is difficult to design compounds that would bind one isozyme with high affinity while all other isozymes with low affinity, thus leading toward high selectivity for only one isozyme. The active site of CAs is funnel-shaped and has hydrophobic and hydrophilic sides for some isozymes. Differences in a few amino acids determine the selectivity of inhibitors for particular isozymes. Introducing various scaffolds on the aromatic sulfonamide ring targets unique residues in the active site.[17] In most studies, the tails are relatively distant from

Received: May 26, 2025
Revised: June 27, 2025
Accepted: July 8, 2025
Published: August 13, 2025

https://doi.org/10.1021/acs.jmedchem.5c01421
J. Med. Chem. 2025, 68, 17752−17773

Scheme 1. Synthesis of Methyl 4-Substituted-3-Sulfamoylbenzoates 4a−d, f−m, 4-Substituted 3-Sulfamoylbenzamides 5a−d, f, g, j−m, and 4-Amino-Substituted Benzamides 6b, c, e[a]

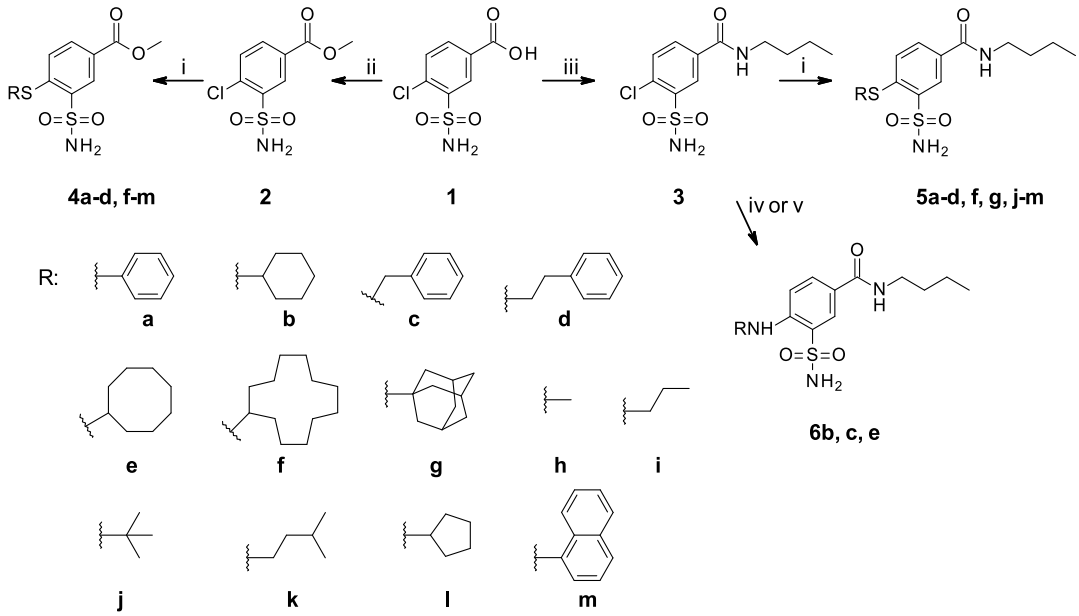

[a]Reagents and conditions: (i) RSH, K_2CO_3, DMF, 80 °C; (ii) H_2SO_4, MeOH, Δ; (iii) (a) $SOCl_2$, toluene, Δ, (b) RNH_2, THF, 0 °C; (iv) RNH_2, 130 °C; (v) RNH_2, TEA, toluene, Δ.

the sulfonamide group, resulting in weak interactions with peripheral amino acids. The affinity profile depended mostly on the substituents located close to the sulfonamide head-group.[18−20] This is also dependent on the flexibility of the substituents, which help adjust to the protein shape.

Depending on the variation of the substituents while investigating doubly substituted compounds,[20−22] several high-affinity compounds exhibiting picomolar K_d were obtained for CAVII, CAIX, CAXII, and CAXIV. A significant achievement was a *LJ15-12* compound that exhibited 0.08 pM intrinsic K_d for CAIX.[20] In this study, we investigate the functional groups in the *ortho* position by varying 13 substituents from small methyl to bulky adamantyl. Sulfinyl and amino substituents were also synthesized to examine the influence of the linking atoms. Interestingly, the substitution of only one atom, an addition of an oxygen atom in the *ortho* position, decreased compound affinity for nontarget isozymes by a million-fold, significantly improving the selectivity, which is one of the main goals in small-molecule drug discovery.

■ RESULTS

Organic Synthesis of Designed Compounds. The synthesis of 2,5-disubstituted benzenesulfonamides was performed starting from 4-chloro-3-sulfamoylbenzoic acid **1** (Scheme 1). Methyl ester **2** was obtained from 4-chloro-3-sulfamoylbenzoic acid **1** by reflux in methanol in the presence of a catalytic amount of sulfuric acid. Amide **3** was synthesized by refluxing acid **1** with thionyl chloride in toluene and subsequent treatment, the resulting anhydride with an appropriate amine, using as the base excess of amine according to the procedure reported in ref 21.

The synthesis of 4-substituted sulfamoylbenzoic acid derivatives **4a−d, f−m** was achieved by aromatic nucleophilic substitution of the chlorine substituent with various thiols under an inert atmosphere in dimethylformamide using potassium carbonate as the base (Scheme 1). All thiols were commercially available except cyclododecylthiol, which was synthesized by subjecting cyclododecanone to reaction with 1,2-ethanedithiol and subsequent reduction of intermediate dithiolane with *n*-butyllithium.[23]

The 4-substituted 3-sulfamoylbenzamides **5a−d, f, g, j−m** were synthesized using the same reaction conditions as 4-sulfanyl-substituted esters **4a−d, f−m**. Substitution of the chlorine group with amines required harsher reaction conditions than thiols. Therefore, 4-amino-substituted benzamides **6b** and **c** were synthesized by heating amide **3** over the appropriate amine at 130 °C. Compound **6e** was synthesized by boiling amide **3** in toluene with 2 equiv of cyclooctylamine and 2 equiv of triethylamine.

The oxidation of esters **4a−d, h, i, k−m** and benzamides **5a, b, k−m** to the sulfinyl and sulfonyl compounds was performed using in situ generated peracetic acid (Scheme 2). The reaction was carried out at room temperature and produced 4-sulfinyl compounds **7a, b, h, i, k−m**, **8a, b, k−m**, and heating the reaction mixture at 70 °C yielded the corresponding 4-sulfonyl compounds **9a−d, h, i, l, m**, **10b**, and **k−m**.

Compound Binding to CA Isozymes. All synthesized compounds were divided into 7 groups: **4(a−d, f−m)**, **5(a−d, f, g, j−m)**, **6(b, c, e)**, **7(a, b, h, i, k−m)**, **8(a, k−m)**, **9(a−d, h, i, l, m)**, and **10(b, k−m)** (Figure 1). Compounds that started with numbers **4**, **7**, and **9** were 4-sulfanyl-, 4-sulfinyl, and 4-sulfonyl-substituted esters, respectively. Compounds starting with the numbers **5**, **8**, and **10** were 4-sulfanyl-, 4-sulfinyl, and 4-sulfonyl-substituted benzamides analogous to the previous series. Compounds starting with the number **6** were 4-amino-substituted benzamides. Various linear, branched, and cyclic aliphatic and aromatic substituents at the *ortho* position were tested to assess whether size, flexibility, and hydrophobicity affect affinity. Compound affinities for the 12 catalytically active human CA isozymes are listed in Table 1.

As one of the important findings in this manuscript, Figure 2 arranges the compounds in the order of their affinity for CAIX

https://doi.org/10.1021/acs.jmedchem.5c01421
J. Med. Chem. 2025, 68, 17752−17773

Scheme 2. Synthesis of Methyl 4-Sulfinyl-Substituted-3-Sulfamoyl Benzoates 7a, b, h, i, k−m, *N*-Butyl-4-sulfinyl-Substituted-3-Sulfamoylbenzamides 8a, b, k−m, Methyl 4-Sulfonyl-Substituted-3-Sulfamoylbenzoates 9a-d, h, i, l, m, and *N*-Butyl-4-sulfonyl-Substituted-3-Sulfamoylbenzamides 10b, k−m[a]

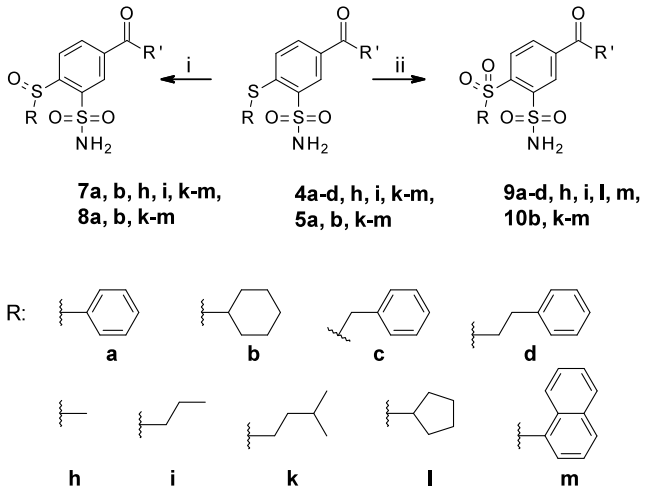

R': OMe (**4**, **7**, **9**); NH-nBu (**5**, **8**, **10**)

[a]Reagents and conditions: (i) 30% H_2O_2, AcOH, r. t.; (ii) 30% H_2O_2, AcOH, 70 °C.

and compared to undesired target CAII. A high affinity for CAIX is desired, because CAIX is implicated in various types of cancer.[24] However, CAII is abundant in erythrocytes, thus an off-target for anticancer inhibitors.

Compound affinities for human CA isozymes were analyzed using fluorescence-based thermal shift assay (FTSA) and the enzymatic activity stopped-flow-based inhibition assay (SFA) (Figure 3). The FTSA determined the observed dissociation constants for all compounds with all 12 CA isozymes (Table 1 and Supplementary Figure S1). From these experimentally determined $K_{d,obs}$, the *intrinsic* dissociation constants $K_{d,int}$ were calculated, and the results are primarily focused on them. Figure 3B,C shows two compounds with strong and weak affinity for CAII and CAIX by FTSA. A single oxygen atom strongly diminished affinity for both isozymes. The stopped-flow assay of CO_2 hydration enzymatic activity inhibition confirmed that the compounds inhibited CAIX and CAII (Figure 3D,E). Inhibition K_i values are presented in Table 2 and Figure S2. The FTSA is a convenient technique covering a significantly wider K_d range than the SFA.[25]

The experimental conditions slightly differed between FTSA and SFA, and it is therefore not appropriate to directly compare the $K_{d,obs}$ and K_i. However, the measured affinities were similar in both techniques. Further analysis is based on FTSA data due to its wider limits in identifying strong binders. Note that the enzyme concentration limits the SFA's ability to determine high-affinity binders. For example, if we use a 10 nM concentration of a CA isozyme, the lowest IC_{50} is 5 nM, half of the protein concentration. Any compound with an IC_{50} stronger than 5 nM would exhibit a dosing curve that appears as an IC_{50} of 5 nM. Thus, compounds that possess single-digit nM or picomolar K_d, cannot be distinguished by SFA.

Sulfonamide binding of CA is a pH-dependent reaction.[6,26,27] The water molecule bound to the CA zinc ion is replaced by the deprotonated form of sulfonamide upon binding.[28,29] The protonation forms required for the interaction exist at different pHs: the CA-Zn(II)-H_2O has the largest fraction at acidic pH and the deprotonated sulfonamide has the largest fraction at alkaline pH. Therefore, the measured affinity is always lower than the intrinsic affinity. The intrinsic parameters are calculated (see equations in the Experimental section) by knowing the pK_a of the CA zinc-bound water and the pK_a of the sulfonamide group (Table 1 and Figure S3). Experimental data of the sulfonamide group pK_a determination for compound **4b** are shown in Figure 4. Figure S3 shows the graphs of pK_a determination for the remaining compounds.

Intrinsic affinities are especially important in rational drug design. It is not rare when a stronger affinity is observed not because of the formed bonds but because of the substitutions that lower the pK_a of the sulfonamide group and thus increase the fraction of the ready-to-bind form.[30] Intrinsic parameters are used to avoid misleading conclusions when comparing the affinity of compounds for CAs.

Esters vs Benzamides. 4-sulfanyl-substituted esters **4a−d**, **f−m** were the largest (12 compounds) studied group of compounds with the same framework. Compounds of this group, even almost independently of the substituent, interacted strongly and selectively with several CAs. $K_{d,int}$ of **4b** for CAIX was 0.0010 nM and it was the strongest interaction measured in this study, CAXIII—0.090 nM and CAXIV—0.020 nM, with others interacting much weaker. The size of the substituent was critical in this interaction. CAIX has a larger active site than the rest of the CAs.[31] It was interesting that compound **4g** (*adamantyl*), which has a similar affinity for CAIX ($K_{d,int}$ =

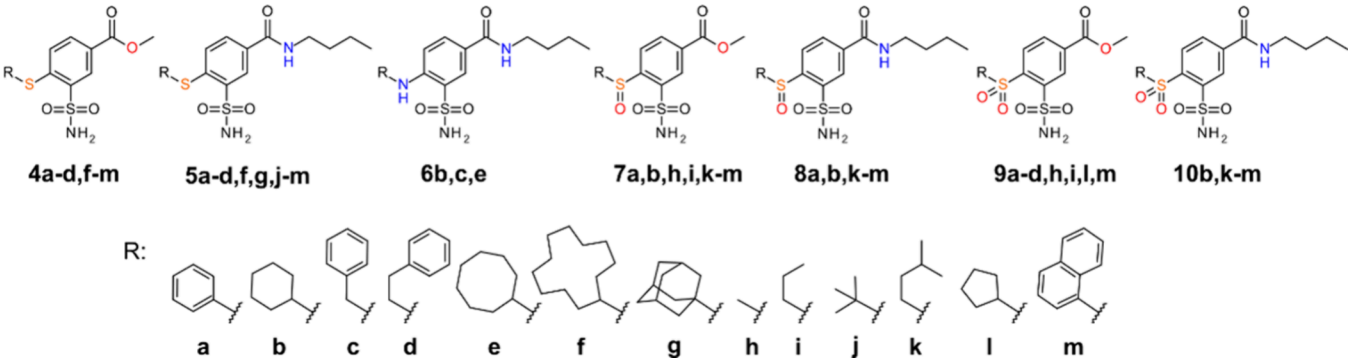

Figure 1. Chemical structures of the compounds synthesized and investigated in this study. Compounds **1**, **2**, and **3** are the starting compounds of the synthesis shown in Scheme 1.

https://doi.org/10.1021/acs.jmedchem.5c01421
J. Med. Chem. 2025, 68, 17752−17773

Table 1. *Observed* and *Intrinsic* ($K_{d,obs}$ and $K_{d,int}$) Dissociation Constants (in nM Units) of Investigated Compounds to All Catalytically Active Human CAs at 37 °C Obtained by Fluorescent Thermal Shift Assay (FTSA)[a]

Compound *lab. name*	A framework of the structure	$pK_{a,SA}$	fraction at pH 7.0		CAI	CAII	CAIII	CAIV	CAVA	CAVB	CAVI	CAVII	CAIX	CAXII	CAXIII	CAXIV
				$pK_{a,CA}$	8.1	6.9	6.5	6.6	7.3	7.0	6.0	6.8	6.6	6.8	8.0	6.8
					92.6%	44.3%	24.0%	28.5%	66.6%	50.0%	9.1%	38.7%	28.5%	38.7%	90.9%	38.7%
2 *JA17-1*	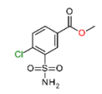	9.2	0.63%	$K_{d,obs}$	21000	460	≥200000	500	770	42	300	240	240	92	220	170
				$K_{d,int}$	120	1.3	≥300	0.90	3.2	0.13	0.17	0.58	0.43	0.22	1.3	0.41
3 *JA17-3*	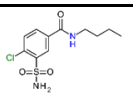	9.1	0.79%	$K_{d,obs}$	36000	140	44000	99	1800	70	340	94	190	10	880	290
				$K_{d,int}$	260	0.50	83	0.22	10	0.28	0.24	0.29	0.43	0.030	6.3	0.89
4a *JA17-1-1*		9.8	0.16%	$K_{d,obs}$	≥200000	87	≥200000	460	≥200000	120	430	140	4.0	260	12	10
				$K_{d,int}$	≥290	0.060	≥76	0.21	≥210	0.10	0.060	0.090	0.0020	0.16	0.020	0.0060
4b *JA17-1-2*		9.7	0.20%	$K_{d,obs}$	≥200000	560	≥200000	810	≥200000	440	710	680	1.8	280	52	22
				$K_{d,int}$	≥370	0.49	≥96	0.46	≥270	0.44	0.13	0.52	0.0010	0.22	0.090	0.020
4c *JA17-1-3*		9.8	0.16%	$K_{d,obs}$	≥200000	590	≥200000	110	140000	930	660	960	10	350	52	90
				$K_{d,int}$	≥290	0.42	≥76	0.050	150	0.70	0.10	0.60	0.0050	0.21	0.080	0.050
4d *JA17-1-4*		9.6	0.25%	$K_{d,obs}$	160000	580	≥200000	1100	97000	190	1300	360	19	450	27	20
				$K_{d,int}$	380	0.64	≥120	0.79	160	0.23	0.29	0.34	0.010	0.43	0.060	0.020
4f *JA18-29*	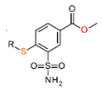	9.7[b]	0.20%	$K_{d,obs}$	≥200000	1000	≥200000	2100	≥200000	1800	6500	18000	11	68	100	100
				$K_{d,int}$	≥370	0.90	≥96	1.2	≥270	1.8	1.2	14	0.0060	0.050	0.18	0.080
4g *E19-3*		9.7[b]	0.20%	$K_{d,obs}$	≥200000	3300	≥200000	100000	≥200000	≥200000	13000	96000	4.8	1500	1200	1200
				$K_{d,int}$	≥370	2.9	≥96	57	≥270	≥200	2.3	74	0.0030	1.1	2.2	1.0
4h *JA19-17*		9.8	0.16%	$K_{d,obs}$	≥200000	2200	≥200000	960	120000	680	500	1000	650	6500	570	440
				$K_{d,int}$	≥290	1.6	≥76	0.43	130	0.54	0.070	0.61	0.29	4.0	0.80	0.27
4i *JA18-30*		9.6	0.25%	$K_{d,obs}$	≥200000	1000	≥200000	400	91000	990	700	490	23	1800	98	70
				$K_{d,int}$	≥460	1.1	≥120	0.28	150	1.2	0.16	0.48	0.020	1.7	0.22	0.070
4j *JA18-33*		9.6	0.25%	$K_{d,obs}$	≥200000	2400	≥200000	10000	≥200000	4900	4600	15000	290	120	220	370
				$K_{d,int}$	≥460	2.7	≥120	7.4	≥330	6.1	1.0	14	0.21	0.12	0.51	0.36
4k *JA18-32*		9.8	0.16%	$K_{d,obs}$	40000	370	≥200000	160	85000	310	300	210	2.7	190	40	33
				$K_{d,int}$	58	0.26	≥76	0.070	89	0.25	0.040	0.13	0.0010	0.11	0.060	0.020
4l *E19-1*		9.6	0.25%	$K_{d,obs}$	≥200000	670	≥200000	1000	180000	6700	560	180	3.3	670	110	20
				$K_{d,int}$	≥460	0.74	≥120	0.71	300	8.4	0.13	0.18	0.0020	0.65	0.25	0.020
4m *E19-2*		9.7	0.20%	$K_{d,obs}$	≥200000	50	11000	2000	≥200000	1300	500	8.7	2.5	500	1.4	25
				$K_{d,int}$	≥370	0.040	5.3	1.1	≥270	1.2	0.090	0.0070	0.0010	0.39	0.0030	0.020
5a *JA17-3-1*		9.7	0.20%	$K_{d,obs}$	≥200000	16000	≥200000	≥200000	120000	9000	19000	53000	360	17000	17000	60000
				$K_{d,int}$	≥370	14	≥96	≥110	160	9	3.5	41	0.20	13	30	46
5b *JA17-3-2*		9.8	0.16%	$K_{d,obs}$	≥200000	180000	100000	≥200000	≥200000	33000	≥200000	≥200000	450	140000	150000	≥200000
				$K_{d,int}$	≥290	120	38	≥90	≥210	26	≥29	≥120	0.20	83	220	≥120
5c *JA17-3-3*		9.8	0.16%	$K_{d,obs}$	≥200000	12000	≥200000	40000	68000	33000	43000	77000	2100	8600	43000	50000
				$K_{d,int}$	≥290	8.1	≥76	18	72	26	6.2	47	0.93	5.3	62	31
5d *JA17-3-4*		9.9	0.13%	$K_{d,obs}$	≥200000	58000	≥200000	≥200000	110000	17000	98000	≥200000	3200	46000	110000	≥200000
				$K_{d,int}$	≥230	32	≥60	≥72	95	10	11	≥97	1.2	22	130	≥97
5f *JA19-16*	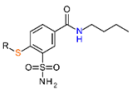	9.8[b]	0.16%	$K_{d,obs}$	≥200000	100000	≥200000	≥200000	≥200000	≥200000	≥200000	≥200000	840	≥200000	≥200000	62000
				$K_{d,int}$	≥290	70	≥76	≥90	≥210	≥160	≥29	≥120	0.38	≥120	≥290	38
5g *YB19-4*		9.8[b]	0.16%	$K_{d,obs}$	≥200000	≥200000	≥200000	≥200000	≥200000	≥200000	≥200000	≥200000	2000	≥200000	≥200000	≥200000
				$K_{d,int}$	≥290	≥140	≥76	≥90	≥210	≥160	≥29	≥120	0.90	≥120	≥290	≥120
5j *YB19-3*		9.8	0.16%	$K_{d,obs}$	≥200000	≥200000	≥200000	≥200000	≥200000	≥200000	≥200000	≥200000	25000	≥200000	≥200000	≥200000
				$K_{d,int}$	≥290	≥140	≥76	≥90	≥210	≥160	≥29	≥120	11	≥120	≥290	≥120

https://doi.org/10.1021/acs.jmedchem.5c01421
J. Med. Chem. 2025, 68, 17752−17773

Table 1. continued

Compound lab. name	A framework of the structure	$pK_{a,SA}$	fraction at pH 7.0		CAI	CAII	CAIII	CAIV	CAVA	CAVB	CAVI	CAVII	CAIX	CAXII	CAXIII	CAXIV
				$pK_{a,CA}$	8.1	6.9	6.5	6.6	7.3	7.0	6.0	6.8	6.6	6.8	8.0	6.8
					92.6%	44.3%	24.0%	28.5%	66.6%	50.0%	9.1%	38.7%	28.5%	38.7%	90.9%	38.7%
5k *YB19-2*	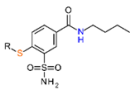	9.7	0.20%	$K_{d,obs}$	≥200000	≥200000	≥200000	≥200000	≥200000	≥200000	≥200000	≥200000	670	≥200000	≥200000	≥200000
				$K_{d,int}$	≥370	≥180	≥96	≥110	≥270	≥200	≥36	≥150	0.38	≥150	≥360	≥150
5l *YB19-5*		9.8	0.16%	$K_{d,obs}$	≥200000	≥200000	≥200000	≥200000	≥200000	≥200000	≥200000	≥200000	800	≥200000	≥200000	≥200000
				$K_{d,int}$	≥290	≥140	≥76	≥90	≥210	≥160	≥29	≥120	0.36	≥120	≥290	≥120
5m *YB19-1*		9.9	0.13%	$K_{d,obs}$	≥200000	≥200000	≥200000	≥200000	≥200000	≥200000	≥200000	≥200000	500	≥200000	10000	≥200000
				$K_{d,int}$	≥230	≥110	≥60	≥72	≥170	≥130	≥23	≥97	0.18	≥97	11	≥97
6b *JA17-3-11*	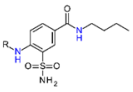	9.8	0.16%	$K_{d,obs}$	180000	20000	≥200000	68000	80000	6500	26000	62000	420	27000	44000	46000
				$K_{d,int}$	260	14	≥76	31	84	5.2	3.7	38	0.19	16	64	28
6c *JA17-3-9*		9.8	0.16%	$K_{d,obs}$	≥200000	22000	≥200000	63000	83000	10000	25000	62000	1500	6500	32000	33000
				$K_{d,int}$	≥290	16	≥76	29	88	8.0	3.6	38	0.66	4.0	47	20
6e *JA17-3-10*		9.8	0.16%	$K_{d,obs}$	≥200000	110000	≥200000	≥200000	190000	≥200000	≥200000	≥200000	1200	64000	150000	20000
				$K_{d,int}$	≥290	79	≥76	≥90	200	≥160	≥29	≥120	0.53	39	220	12
7a *JA19-11*	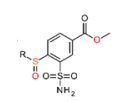	8.9[b]	1.24%	$K_{d,obs}$	≥200000	340	93000	900	≥200000	910	970	79	130	2900	120	99
				$K_{d,int}$	≥2300	1.8	280	3.2	≥1700	5.6	1.1	0.38	0.45	14	1.3	0.48
7b *JA19-10*		8.9	1.24%	$K_{d,obs}$	≥200000	≥200000	≥200000	≥200000	≥200000	≥200000	≥200000	≥200000	7800	≥200000	≥200000	≥200000
				$K_{d,int}$	≥2300	≥1100	≥600	≥710	≥1700	≥1200	≥230	≥960	28	≥960	≥2300	≥960
7h *JA19-19*		8.9	1.24%	$K_{d,obs}$	≥200000	4300	≥200000	5500	≥200000	33000	1200	18000	5200	15000	720	3300
				$K_{d,int}$	≥2300	24	≥600	19	≥1700	200	1.3	87	18	74	8.1	16
7i *JA19-3*		8.9	1.24%	$K_{d,obs}$	≥200000	≥200000	≥200000	≥200000	100000	≥200000	111000	≥200000	43000	≥200000	26100	45000
				$K_{d,int}$	≥2300	≥1100	≥600	≥710	830	≥1200	130	≥960	150	≥960	290	220
7k *JA19-8*		8.8	1.56%	$K_{d,obs}$	≥200000	2400	≥200000	9000	≥200000	14000	13000	9300	140	7600	400	2000
				$K_{d,int}$	≥2900	16	≥750	40	≥2100	110	18	56	0.63	46	5.6	12
7l *E19-6*		8.9	1.24%	$K_{d,obs}$	27000	3600	≥200000	12000	≥200000	130000	9800	68000	200	18000	1600	510
				$K_{d,int}$	310	20	≥600	42	≥1700	780	11	330	0.72	86	18	2.5
7m *E19-7*		9.1	0.79%	$K_{d,obs}$	52000	2900	≥200000	1200	≥200000	58000	65000	5400	110	2600	700	180
				$K_{d,int}$	380	10	≥380	2.8	≥1000	230	47	16	0.24	8.1	5.0	0.54
8a *JA19-15*	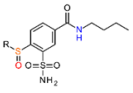	9.0	0.99%	$K_{d,obs}$	180000	13000	≥200000	50000	≥200000	13000	≥200000	100000	14000	≥200000	50000	≥200000
				$K_{d,int}$	1600	55	≥480	140	≥1300	62	≥180	380	40	≥770	450	≥770
8k *YB19-10*		9.0	0.99%	$K_{d,obs}$	≥200000	160000	≥200000	≥200000	≥200000	≥200000	≥200000	≥200000	3300	≥200000	180000	≥200000
				$K_{d,int}$	≥1800	710	≥480	≥560	≥1300	≥990	≥180	≥770	9	≥770	1600	≥770
8l *YB19-11*		9.0[b]	0.99%	$K_{d,obs}$	33000	14000	≥200000	≥200000	≥200000	≥200000	≥200000	≥200000	13000	≥200000	≥200000	10000
				$K_{d,int}$	310	63	≥480	≥560	≥1300	≥990	≥180	≥770	35	≥770	≥1800	38
8m *YB19-7*		8.9	1.24%	$K_{d,obs}$	≥200000	141800	≥200000	≥200000	≥200000	≥200000	≥200000	≥200000	4600	≥200000	146300	≥200000
				$K_{d,int}$	≥2300	780	≥600	≥710	≥1700	≥1200	≥230	≥960	16.0	≥960	1700	≥960
9a *JA17-1-5*	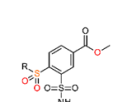	9.0	0.99%	$K_{d,obs}$	≥200000	56000	≥200000	≥200000	≥200000	≥200000	110000	57000	76000	≥200000	16000	42000
				$K_{d,int}$	≥1800	250	≥480	≥560	≥1300	≥990	94	220	220	≥770	140	160
9b *JA17-1-7*		8.9	1.24%	$K_{d,obs}$	≥200000	≥200000	≥200000	≥200000	≥200000	≥200000	≥200000	28000	90000	≥200000	100000	140000
				$K_{d,int}$	≥2300	≥1100	≥600	≥710	≥1700	≥1200	≥230	130	320	≥960	1100	680
9c *JA17-1-8*		8.9	1.24%	$K_{d,obs}$	≥200000	≥200000	≥200000	68000	≥200000	≥200000	≥200000	70000	11000	≥200000	56000	29000
				$K_{d,int}$	≥2300	≥1100	≥600	240	≥1700	≥1200	≥230	340	37	≥960	640	140
9d *JA17-1-6*		9.0	0.99%	$K_{d,obs}$	≥200000	≥200000	≥200000	140000	≥200000	≥200000	160000	≥200000	≥200000	≥200000	25000	54000
				$K_{d,int}$	≥1800	≥880	≥480	390	≥1300	≥990	150	≥770	≥560	≥770	220	210
9h *JA19-20*		8.8	1.56%	$K_{d,obs}$	≥200000	82000	≥200000	89000	140000	≥200000	64000	160000	73000	170000	22000	59000
				$K_{d,int}$	≥2900	570	≥750	400	1400	≥1600	91	960	320	1100	310	350

https://doi.org/10.1021/acs.jmedchem.5c01421
J. Med. Chem. 2025, 68, 17752−17773

Table 1. continued

Compound lab. name	A framework of the structure	$pK_{a,SA}$	fraction at pH 7.0		CAI	CAII	CAIII	CAIV	CAVA	CAVB	CAVI	CAVII	CAIX	CAXII	CAXIII	CAXIV
				$pK_{a,CA}$	8.1	6.9	6.5	6.6	7.3	7.0	6.0	6.8	6.6	6.8	8.0	6.8
					92.6%	44.3%	24.0%	28.5%	66.6%	50.0%	9.1%	38.7%	28.5%	38.7%	90.9%	38.7%
9i *JA19-2*	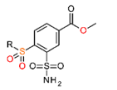	8.9	1.24%	$K_{d,obs}$	≥200000	1700	≥200000	6200	≥200000	9000	1500	≥200000	900	16000	250	920
				$K_{d,int}$	≥2300	10	≥600	22	≥1700	56	1.7	≥960	3.2	76	2.8	4.4
9l *E19-4*		9.0	0.99%	$K_{d,obs}$	≥200000	71000	≥200000	190000	≥200000	≥200000	≥200000	≥200000	9100	≥200000	22000	20000
				$K_{d,int}$	≥1800	310	≥480	540	≥1300	≥990	≥180	≥770	26	≥770	200	78
9m *E19-5*		9.0	0.99%	$K_{d,obs}$	≥200000	5900	≥200000	≥200000	≥200000	≥200000	35000	6800	4000	≥200000	630	6300
				$K_{d,int}$	≥1800	26	≥480	≥560	≥1300	≥990	31	26	11	≥770	5.6	24
10b *JA19-14*	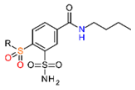	9.0	0.99%	$K_{d,obs}$	≥200000	≥200000	≥200000	≥200000	≥200000	≥200000	≥200000	≥200000	≥200000	≥200000	≥200000	≥200000
				$K_{d,int}$	≥1800	≥880	≥480	≥560	≥1300	≥990	≥180	≥770	≥560	≥770	≥1800	≥770
10k *YB19-8*		9.0	0.99%	$K_{d,obs}$	≥200000	≥200000	≥200000	≥200000	≥200000	≥200000	≥200000	≥200000	≥200000	≥200000	≥200000	160000
				$K_{d,int}$	≥1800	≥880	≥480	≥560	≥1300	≥990	≥180	≥770	≥560	≥770	≥1800	620
10l *YB19-9*		9.1	0.79%	$K_{d,obs}$	≥200000	≥200000	≥200000	≥200000	≥200000	150000	≥200000	≥200000	≥200000	≥200000	≥200000	≥200000
				$K_{d,int}$	≥1500	≥700	≥380	≥450	≥1000	610	≥140	≥610	≥450	≥610	≥1400	≥610
10m *YB19-6*		8.9	1.24%	$K_{d,obs}$	≥200000	≥200000	≥200000	≥200000	≥200000	≥200000	≥200000	≥200000	≥200000	≥200000	≥200000	≥200000
				$K_{d,int}$	≥2300	≥1100	≥600	≥710	≥1700	≥1200	≥230	≥960	≥710	≥960	≥2300	≥960
AZM		7.0	50%	$K_{d,obs}$	2400	46	40000	87	840	140	220	13	21	130	79	63
				$K_{d,int}$	1100	9.8	4600	12	270	34	9.8	2.4	2.9	24	35	12

[a]Observed values were determined using 50 mM sodium phosphate buffer at pH 7.0 containing 100 mM sodium chloride, 50 μM ANS dye, and 2% (v/v) DMSO. $K_{d,int}$s were calculated according to eq 1 (see the Experimental Section). Values with a "≥" sign show that they are at the detection limit of ≥200 000 nM of $K_{d,obs}$ according to the highest used ligand concentration. The intrinsic value limits vary for different CAs and compounds due to differences in pK_a. $pK_{a,SA} - pK_a$ of the sulfonamide group; $pK_{a,CA} - pK_a$ value of water molecule bound to Zn(II) in the active site of CA; AZM, acetazolamide (a standard inhibitor). [b]Not determined due to solubility issues or low intensity of the spectrum curves. The $pK_{a,SA}$ value was assigned based on similarities in chemical structure.

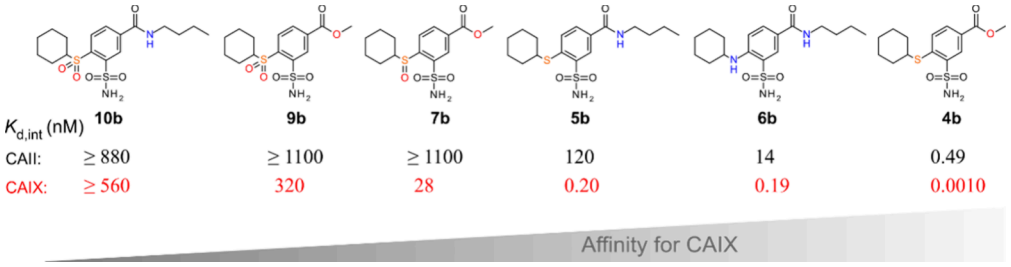

Figure 2. Compounds are arranged in the order of increasing affinity for CAIX. Compound **4b** had the highest affinity and selectivity for CAIX. The intrinsic dissociation constants (in nM units) are compared for CAII and CAIX, while values for the remaining CAs are listed in Table 1.

0.0030 nM) to most of the compounds in this group, is a few hundred times more selective for CAIX, whereas, for example, **4b** (*cyclohexyl*) is only a few tens of times more selective for CAIX and can be considered a strong binder to several undesired CAs. On the other hand, the 4-methylsulfanyl- substituted compound **4h** is no longer selective. Thus, the hydrophobic interaction made a significant contribution to affinity for CAIX, and selectivity was mainly obtained by the size of the substituent when the binding to CAIX was optimal and binding to other CAs was limited by steric interference. Analogous benzamides were much weaker binders of CAs. Most benzamides exhibited no interaction with CAs. Nevertheless, all compounds in this series bound to CAIX and were, in most cases, at least several dozen times more selective for it than for other CAs.

Sulfanyl vs Sulfinyl vs Sulfonyl Compounds. Different forms of sulfur oxidation led to drastically different affinities for CAs. A higher degree of oxidation in these compounds weakened the affinity. However, in our opinion, it was not the oxidation itself that had the main influence, but rather the conformation of the compound. The affinity of all sulfinyl- compounds with all CAs was significantly weaker than analogous sulfanyl- compounds. The decrease in affinity varied depending on the CA isozyme and the substituents. Therefore, no generalized observations could be made. For example, compound **7a** did not bind to CAI and CAVA, but the weak affinity was determined for CAIII, with all other CAs the interactions were similar and did not exceed more than 10-fold in most cases and there was no selectivity for CAIX. Compounds **7b**, **7h**, and **7i** did not bind or bind weakly and nonselectively to all CAs. Except for **7b**, it is bound only to CAIX with 28 nM. The $K_{d,int}$ of compounds **7k**, **7l**, and **7m** were 0.63, 0.72, and 0.24 nM, respectively. Also, there was a similar affinity for CAXIII and CAXIV and weaker for the other CAs. From compounds **5(a−d, f, g, j−m)** to **8(a, k−m)** decreased affinity for all CAs.

https://doi.org/10.1021/acs.jmedchem.5c01421
J. Med. Chem. 2025, 68, 17752−17773

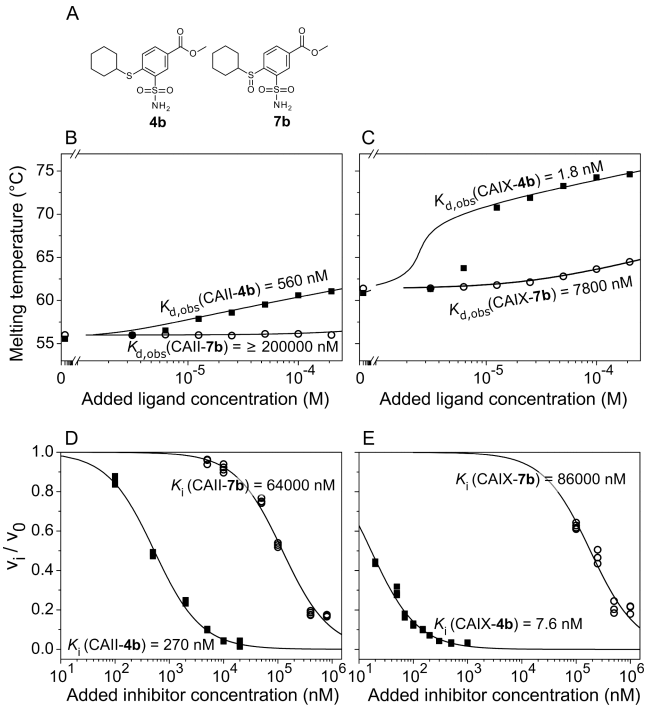

Figure 3. Compound affinity was determined by two assays in this study. (A) Chemical structures of two compounds whose binding data are shown below. (B) and (C) Fluorescent thermal shift assay data (FTSA) of compounds **4b** (closed squares) and **7b** (open circles) binding to CAII and CAIX, respectively. (D) and (E) Stopped-flow carbon dioxide hydration assay (SFA) data of compounds **4b** (closed squares) and **7b** (open circles) inhibition of CAII and CAIX, respectively. The dissociation constants (K_d) or inhibition constants (K_i) are given next to the corresponding curves. It is important to note that the experimental conditions of the methods were slightly different: FTSA, pH 7.0, 37 °C, while for SFA, pH 7.5, 25 °C.

Switching to sulfonyl compounds reduced the affinity and abolished the selectivity for CAIX. **9b** only bound to CAVII, CAIX, CAXIII, and CAXIV with $K_{d,int}$ 130, 320, 1100, and 680 nM, respectively. The most strongly interacting compound in this series was **9i**, e.g., $K_{d,int}$ of CAVI—1.7 nM, CAIX—3.2 nM but also bound to other CAs quite similarly. Meanwhile, compounds **10(b, k−m)** did not bind to any isozymes, only a couple of measurements showed a weak interaction.

4-Sulfanyl- vs 4-Amino-Substituted. Comparing **5b** vs. **6b** and **5c** vs. **6c**, in most cases, the dissociation constants differed only a few times, and the constants for CAIX did not exceed the margin of error. The S or N atom in the same position of the compound almost did not change the affinity for all isozymes. Compound **6e** (cyclooctyl-substituted) selectively interacted with CAIX, $K_{d,int}$ of CAIX—0.53 nM, CAXII—39 nM, and CAXIV—12 nM. It did not bind to other CAs. Most likely the selectivity was due to the size of the active site pocket.

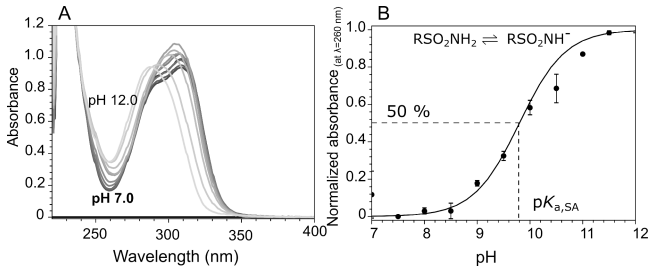

Figure 4. Spectrophotometric determination of the sulfonamide group deprotonation pK_a for compound **4b**. (A) Absorption spectra of compound **4b** in solutions at various pH at intervals of 0.5 pH units at 37 °C. (B) Normalized absorbance at 260 nm was plotted as a function of pH, and the pK_a value was determined as a midpoint of the curve. The data points are the mean points of two repeats ((A) shows one repeat for simplicity), with standard deviations. The pK_a value of compound **4b** was 9.74 ± 0.13 (±1.3%) with a confidence interval [9.62−9.87] of 95%.

X-ray Crystal Structures of Compound Binding to CAII and CAXIII. Nine crystal structures were determined by X-ray crystallography, the complexes of CAII with compounds **2**, **3**, **4c**, **4d**, **4h**, CAIX with **4d** and **5b**, and CAXIII with **4c** and **4d**. Table 3 lists the data collection and refinement statistics. Figure 5 shows the electron density maps of these compounds in the active site of CAs. Two molecules of compound **4h** were identified in the active site of CAII, one conventionally formed a coordination bond between the sulfonamide group and zinc, and the other was independently located near the periphery of the active site. The localization of both separated molecules relative to the same zinc is shown in Figure 5E,F. The main highlights of the identified protein−ligand interactions are described below and illustrated in Figure 6.

*Structures of **2** vs **3** Bound to CAII.* Starting compounds **2** and **3** used in the synthesis differed by one substitution at the *meta* position relative to the sulfonamide group, ester vs. amide. Figure 6A,B shows the position of these compounds in the active site of CAII. Both compounds retained the same position of the sulfonamide group and the chlorine atom in the active site of

Table 2. Inhibition Constants and IC_{50} (in nM Units) of CAII and CAIX with Compounds Obtained by Stopped-Flow Carbon Dioxide Hydration Assay (SFA) at 25 °C[a]

	K_i (nM)		IC_{50} (nM)	
compound	CAII	CAIX	CAII	CAIX
4a	25 ± 1.3	5.4 ± 0.5	47 ± 2.6	12 ± 0.5
4b	270 ± 20	7.6 ± 0.5	530 ± 40	16 ± 1.3
4c	210 ± 30	37 ± 3.5	400 ± 50	79 ± 7
4d	120 ± 10	51 ± 6	230 ± 20	110 ± 12
4h	9200 ± 500	1300 ± 200	18,000 ± 1000	2700 ± 400
7a	63 ± 6	360 ± 30	120 ± 12	760 ± 60
7b	64,000 ± 7500	86,000 ± 16,000	100,000 ± 10,000	200,000 ± 30,000
7h	3400 ± 200	7600 ± 700	6500 ± 300	16,000 ± 1600
9a	34,000 ± 4000	3700 ± 600	65,000 ± 7000	7800 ± 1300

[a]Experiments were performed using 20 mM HEPES Na at pH 7.5, 20 mM Na_2SO_4, and 0.2 mM Phenol Red.

https://doi.org/10.1021/acs.jmedchem.5c01421
J. Med. Chem. 2025, 68, 17752−17773

Table 3. X-ray Diffraction Data Collection and Refinement Statistics

isozyme—ligand	CAII—**2**	CAII—**3**	CAII—**4c**	CAII—**4d**	CAII—**4h**	CAIX—**4d**	CAIX—**5b**	CAXIII—**4c**	CAXIII—**4d**
PDB ID	9FPT	9FPU	9FPQ	9FPR	9FPS	9R8X	9R8Y	9FPV	9FPW
				Data Collection Statistics					
space group	$P12_11$	$P12_11$	$P12_11$	$P12_11$	$P12_11$	H3	H3	$P2_12_12_1$	$P2_12_12_1$
unit-cell parameters (a, b, c (Å); α, β, γ (°))	a = 42.1, b = 40.9, c = 71.7, $\alpha = \gamma$ = 90, β = 104.0	a = 42.0, b = 41.1, c = 71.9, $\alpha = \gamma$ = 90, β = 104.2	a = 42.3, b = 41.3, c = 72.2, $\alpha = \gamma$ = 90, β = 104.2	a = 42.3, b = 41.3, c = 72.1, $\alpha = \gamma$ = 90, β = 104.5	a = 42.3, b = 41.2, c = 72.0, $\alpha = \gamma$ = 90, β = 104.4	$a = b$ = 152.5, c = 172.4, $\alpha = \beta$ = 90, γ = 120	$a = b$ = 151.9, c = 173.7, $\alpha = \beta$ = 90, γ = 120	a = 55.1, b = 58.0, c = 160.2, $\alpha = \beta = \gamma$ = 90	a = 55.5, b = 58.4, c = 160.7, $\alpha = \beta = \gamma$ = 90
resolution range (Å)	69.6−1.2	40.7−1.1	70.0−1.5	40.0−1.5	39.9−1.4	47.95−2.0	47.8−1.95	80.1−1.7	40.2−1.9
unique reflections number	75321	87594	38824	41447	47284	101012	108927	57402	42102
R_{merge}, overall (outer shell)	0.04 (0.38)	0.05 (0.31)	0.05 (0.25)	0.05 (0.39)	0.04 (0.38)	0.08 (1.18)	0.21 (1.30)	0.09 (0.32)	0.12 (0.31)
I/σ overall (outer shell)	16.9 (3.5)	13.7 (3.8)	15.9 (4.9)	19.6 (4.6)	24.2 (4.7)	21.1 (2.3)	7.1 (1.5)	16.8 (7.4)	13.0 (7.6)
multiplicity overall (outer shell)	6.8 (6.7)	6.6 (6.0)	6.6 (6.4)	7.0 (6.9)	7.0 (6.8)	10.4 (10.5)	10.4 (9.9)	13.2 (13.1)	13.1 (13.4)
completeness (%) overall (outer shell)	96.7 (94.0)	96.0 (91.3)	99.6 (99.2)	98.7 (97.7)	97.6 (94.9)	100.0 (100.0)	100.0 (100.0)	100 (100)	100 (100)
Wilson B-factor	12.8	11.4	17.8	15.5	17.0	28.0	22.4	16.9	22.5
				Refinement Statistics					
R_{work}	0.14	0.15	0.17	0.14	0.14	0.17	0.21	0.16	0.19
R_{free}	0.18	0.17	0.20	0.21	0.19	0.21	0.25	0.19	0.23
RMSD bond lengths (Å)/ angles (°)	0.02/2.13	0.02/2.26	0.01/1.80	0.01/2.04	0.01/2.02	0.01/1.81	0.01/1.73	0.01/1.90	0.01/1.57
average B factors (Å^2): all atoms/inhibitors	22.7/17.2	19.6/16.9	21.6/21.9	20.1/15.7	21.8/21.7	31.9/50.4	30.7/39.4	21.6/32.5	25.9/35.6
Ramachandran statistics (%): favored/allowed/outliers	97/3/ 0	97/3/ 0	97/3/ 0	96/4/ 0	96/4/ 0	96/4/ 0.11	94/5/ 0.32	chain A: 98/2/ 0 chain B: 97/3/ 0	chain A: 97/3/ 0 chain B: 97/3/ 0

https://doi.org/10.1021/acs.jmedchem.5c01421
J. Med. Chem. 2025, 68, 17752−17773

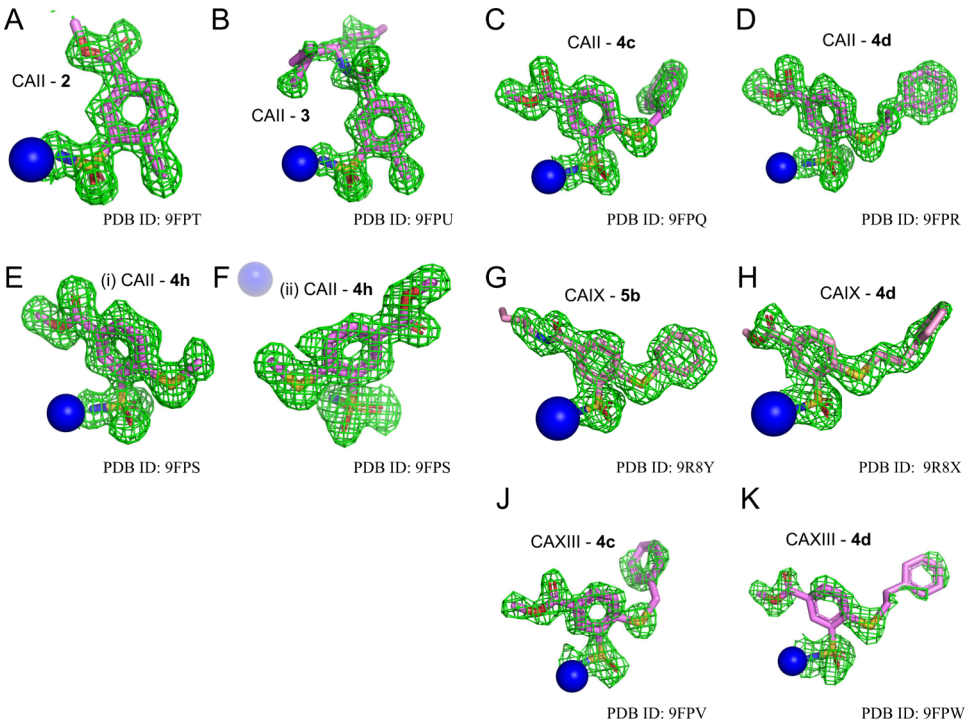

Figure 5. $|F(o) - F(c)|$ omit maps at 3σ in green for the investigated ligands in the active site of CAs. (A) CAII—**2** (PDB ID: 9FPT), (B) CAII—**3** (PDB ID: 9FPU), (C) CAII—**4c** (PDB ID: 9FPQ), (D) CAII—**4d** (PDB ID: 9FPR), (E) and (F) CAII—**4h** (PDB ID: 9FPS; two ligand molecules were identified, one bound directly to Zn in a conventional position, while the second was seen located nearby toward the edge of the active site), (G) CAIX—**5b** (PDB ID: 9R8Y), (H) CAIX—**4d** (PDB ID: 9R8X), (**J**) CAXIII—**4c** (PDB ID: 9FPV), (**K**) CAXIII—**4d** (PDB ID: 9FPW). Omit maps were taken from a refinement run of the final model without the ligand. Zinc is shown in blue.

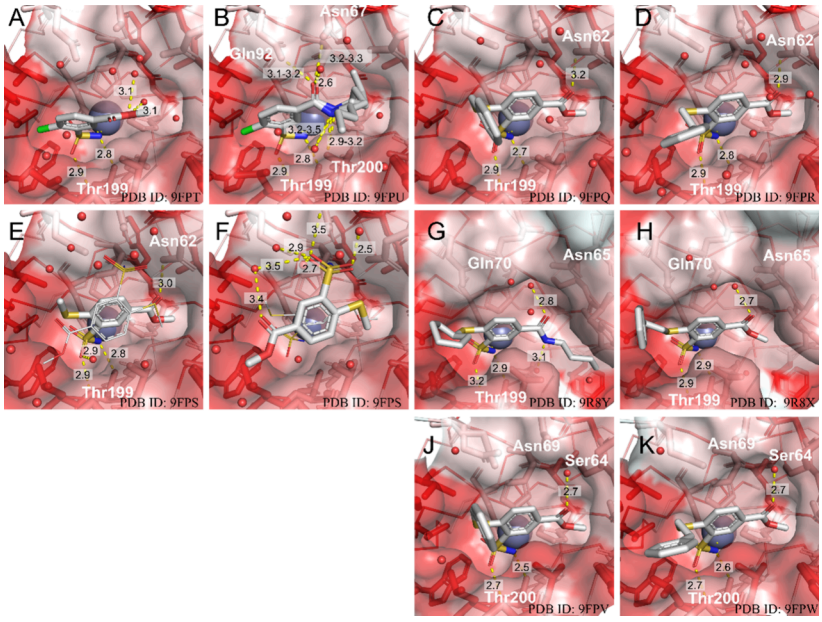

Figure 6. X-ray crystal structures of (A) CAII—**2** (PDB ID: 9FPT), (B) CAII—**3** (PDB ID: 9FPU), (C) CAII—**4c** (PDB ID: 9FPQ), (D) CAII—**4d** (PDB ID: 9FPR), (E) and (F) CAII—**4h** (PDB ID: 9FPS; two ligand molecules were identified, one bound directly (E) to Zn in a conventional position, while the second is seen located nearby toward the edge (F) of the active site), (G) CAIX—**5b** (PDB ID: 9R8Y), (H) CAIX—**4d** (PDB ID: 9R8X), (**J**) CAXIII—**4c** (PDB ID: 9FPV), (**K**) CAXIII—**4d** (PDB ID: 9FPW). The yellow dashed line represents the hydrogen bond; the distances are given in angstroms. The amino acids directly involved in hydrogen bond formation are labeled. Amino acids are colored according to hydrophobicity:[32] the most intense red color represents the most hydrophobic amino acids.

CAII. The amide substituent formed multiple hydrogen bonds with the amino acid side groups, while the ester was stabilized by a network of hydrogen bonds through water molecules. Presumably, a different network of hydrogen bonds pulled the entire molecule slightly, so a partially rotated benzene ring was observed in the crystal structure. No significant conformational changes were observed in the amino acid chains of the active site of CAII. However, the amide substituent of the compound was

https://doi.org/10.1021/acs.jmedchem.5c01421
J. Med. Chem. 2025, 68, 17752−17773

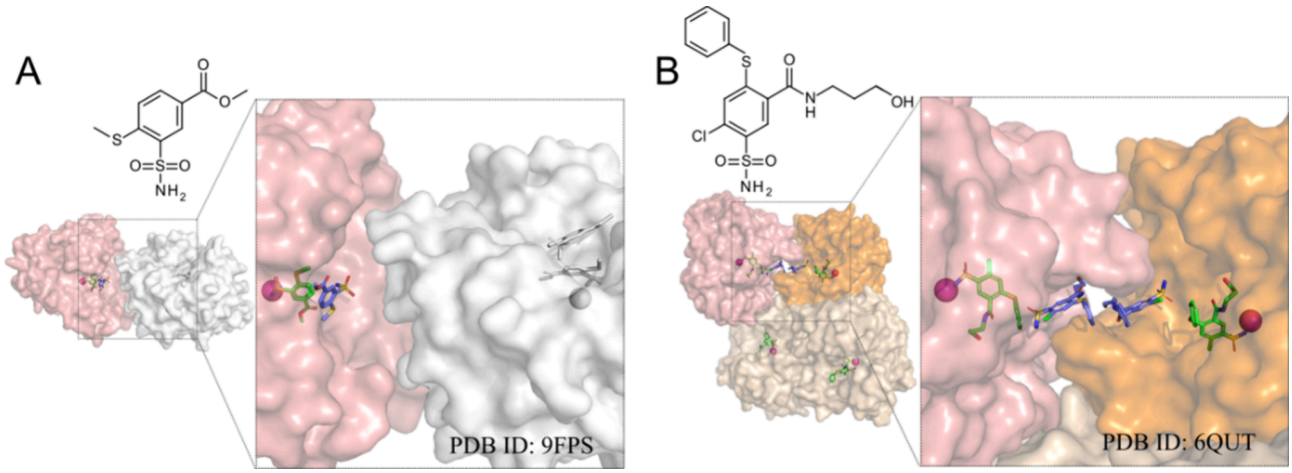

Figure 7. Unusual ligand positions in crystal structures of CAII (PDB ID: 9FPS) and CAIX (PDB ID: 6QUT, published previously[2]). The chemical structures of the ligands are shown above the crystal structures. The crystal structures represent a view of the monomers and a zoomed-in view of the active site. Zn(II) is shown as a pink sphere. Bound to Zn(II) inhibitor molecules are green and others are blue. (A) Monomer of CAII is shown in surface mode and colored salmon. The symmetric chain is colored white. (B) In the case of CAIX, only the asymmetric unit is represented. Six inhibitor molecules are bound to 4 CA IX chains. Chain C (orange) and chain D (salmon) have two inhibitor molecules, and chains A and B (beige) have one molecule. In this case, the interaction of ligands between separate chains is visible.

not in one fixed position. Instead, 3 alternative conformations of the substituent were identified in the structure. However, it should be noted that this substituent has a poor electron density, likely due to its high flexibility. Consequently, its exact arrangement cannot be determined.

*Structures of CAII with Chlorine-Substituted (**2**, **3**) vs Sulfanyl-Substituted (**4c**, **4d**, and **4h**).* The position of *ortho-sulfanyl* and chlorine-substituted compounds in the CAII active site differed significantly. The entire sulfanyl-substituted molecule was shifted to avoid steric interference but maintained a similar distance between the sulfonamide group's nitrogen and the enzyme's zinc compared to the chlorine-substituted compound. Meanwhile, the studied *ortho*-substituted compounds occupied similar positions, and the ester groups of all three compounds formed a hydrogen bond with Asn62. Notably, the electron density of all inhibitor molecules is well-defined.

*Structures of CAII vs CAIX and CAXIII with Bound Sulfanyl-Substituted (**4c** and **4d** or **5b**).* Figure 6 shows the interactions between CAII with compounds **4c** and **4d** (Figure 6C,D), CAIX with **4d** (Figure 6H), and CAXIII with compounds **4c** and **4d** (Figure 6J,K). One of the main differences was in the formed hydrogen bonds. The oxygen of the ester group of the compound formed a direct hydrogen bond with Asn62 in the active site of CAII. Meanwhile, a hydrogen bond is formed in the active site of CAIX and CAXIII through a water molecule with Gln70 and Asn65 or Ser64 and Asn69, respectively. Asn62 in CAII, Asn65 in CAIX, and Asn69 in CAXIII differ only by the numbering but correspond to the same position.

Incidentally, compound **5b** CAIX also forms the same hydrogen bond through a water molecule, and the entire molecule adopts a similar conformation. Notably, the electron density of the 17 amino acids at the N-terminus of both X-ray crystal structures of CAIX is not defined as expected. These amino acids fold in their 3D structure to form the active site of the protein. This side of the active site is called the hydrophilic part. This suggests that the bound ligand pushes these amino acids to fit fully into the active site. When comparing these structures (PDB ID: 9R8X and 9R8Y) with those existing in the PDB (e.g., PDB ID: 3iai), the clash between ligand and Tyr7 is seen without changing their arrangement.

It is important to emphasize that both **4c** and **4d** have very poor electron density in the CAXIII active center, so the arrangement of the compound should be evaluated more cautiously. On the other hand, a comparison of the structures shows that compound **4d** is more similarly located in the active sites of CAII and CAXIII, while in CAIX, it is shifted toward the hydrophilic side, which, as mentioned, is not fully visible in the X-ray structure.

Atypical Binding Position. The structure 9FPS was unique because two ligand molecules were identified as bound in the active site. One molecule was bound classically and formed a coordination bond with the zinc ion. The second formed a hydrophobic interaction with the first molecule, and hydrogen bonds with water molecules located toward the edge of the active site. This could be a crystallographic artifact or a secondary interaction with the protein.[33] A previous publication[2] identified a similar case with CAIX (PDB ID: 6QUT) (Figure 7). In that case, the molecules interacted in the active site and among themselves between the chains in an asymmetric unit. This case with CAII was different because the two chains had no interaction between ligand molecules. The active sites of symmetric chains were not oriented face-to-face. The atoms of the second nonclassical ligand were further than 5Å from the amino acids of the symmetric chain.

Molecular Docking. To understand the differences in the binding affinities of series **4**, **7**, and **9** ligands, they were docked into CAII, except for **4e** and **4f**, containing large, flexible rings that are challenging to dock. Series **4** ligands were also docked into CAIX and CAXIII, to compare with crystal structures and thus assess the docking accuracy. To reduce bias, different receptors (PDB IDs − CAII: 3HS4; CAIX: 6G9U, chain A; CAXIII: 4KNN, chain A) were chosen instead of the new X-ray structures presented in this paper.

To mimic the donor−acceptor bond between the zinc ion and the sulfonamide nitrogen of the ligand, we employed constrained docking using the Smina program.[34] The constraint forced the sulfonamide nitrogen to maintain its original position in the X-ray structure. The generated poses were afterward

https://doi.org/10.1021/acs.jmedchem.5c01421
J. Med. Chem. 2025, 68, 17752−17773

rescored using the Vinardo scoring function.[35] Vina[36] and GNINA[37] Machine-learning-based scoring functions were found to be inferior to Vinardo for this system, and therefore only the latter was employed for further analysis. The pose with the best rescored affinity that matched the X-ray conformation of the benzenesulfonamide moiety was then chosen as the representative best docked structure (in all cases, for ligand **4** series, it was ranked 1 by Vinardo, except for **4j**, where the correct benzenesulfonamide conformation was ranked 3). The best docked poses for CAII are shown in Figure 8A. The Pearson

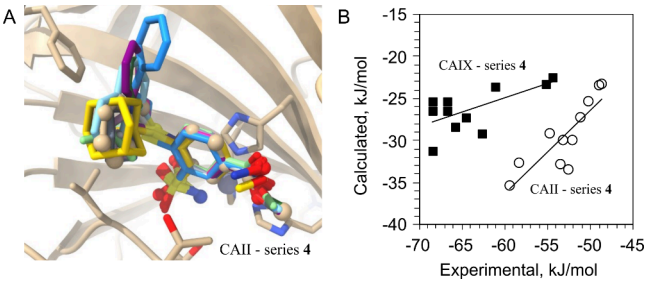

Figure 8. (A) Docked series **4** ligands (see main text for details) superposed onto the X-ray structure of **4c** (PDB ID: 9FPQ; rendered using ball-and-stick representation) in a complex with CAII. Note that hydrophobic substituents stack against the Phe131 side chain. (B) Computed ligand binding affinities to CAII (circles) and CAIX (squares) using Vinardo scoring function plotted against the experimental binding affinities—intrinsic Gibbs energy changes. The Pearson correlations R of the plotted points are 0.87 for CAII and 0.66 for CAIX. The large difference between the computed and experimental binding affinities is because the Vinardo scoring function does not take into account the interaction with zinc. However, it can be assumed to be approximately equal for all ligands.

correlation coefficient R with the experimental *intrinsic* binding affinities to CAII for the best docked poses was 0.87. Figure 8B plots the corresponding computed and experimental binding affinities for CAII and CAIX (values listed in Table S1 in the Supporting Information). Notably, for CAII, the scoring function correctly predicts the best binder, **4m**, and the four worst binders (**4g**−**j**). The panel also shows the correspondence between the experimental and predicted binding affinities for CAIX, with $R = 0.66$.

Validation of the Docking Protocol via Comparison with the X-ray Structures. The proposed docking and scoring protocol was further validated by comparing the predicted docked poses of some of the ligands with their conformations in the newly reported X-ray structures. Figure S4A−C shows the ranked poses of ligands **4c**, **4d**, and **4h** compared against their X-ray conformations in the complex with CAII. The heavy atom Root Mean Square Deviation (RMSD) between the docked and X-ray conformation is 2.03, 3.13, and 0.46 Å, respectively. For the first two ligands, however, the rank 2 conformations are close to the X-ray conformation (**4c**: 0.61 Å; **4d**: 0.67 Å, see Figure S4A,B).

To further validate the chosen docking protocol, **4d** and **5b** were docked into CAIX (PDB ID: 6G9U, chain A). The best-scored poses after reranking using Vinardo are shown in Figure S5. The corresponding heavy atom RMSDs for **4d** and **5b** are 2.18 and 0.92 Å, respectively, and despite the RMSD for **4d** being above 2 Å, the binding mode is captured by the docking reasonably well, especially since the receptor used for docking was originally bound to a ligand from a chemically different series.

Compounds **4c** and **4d** were also docked into the CAXIII receptor (PDB ID: 4KNN, chain A). Similarly to CAIX, the docking protocol picked the docked pose with the approximately correct binding mode (with RMSDs equal to 1.90 and 0.95 Å, respectively) (Figure S6).

Docking of Series 7 and 9 Compounds. Since series **4** compounds using the docking protocol described above can reproduce the scaffold rather well and generally seem to stack the hydrophobic substituents reasonably, we applied a similar procedure by docking series **9** ligands into CAII as a model protein, in hopes that it will help to explain a difference between the binding affinities of series **4** and **9**. Docking using the same protocol led to comparable binding affinities between the two series (not shown). However, experiments indicate that **9** binds worse by several orders of magnitude, and rescored constrained pose affinities for this series exhibit practically no correlation with the experiment ($R \cong 0.12$). A careful examination of the docking results for series **9** revealed the source of the poor binding affinities and the poor performance of the docking score. Figure 9A displays the best ranking pose of **9a**. While the phenyl substituent of **9a** stacks well with Phe131 side chain, the two sulfonyl moieties exhibit an apparent clash against each other.

To further explore this clash, we ran simulations of a simple compound 2-(methylsulfonyl)benzenesulfonamide containing sulfonamide and methylsulfonyl groups at the *ortho*-positions on a benzene ring. The lowest energy conformer for this compound was generated using CREST software[38] using semiempirical GFN2-xTB wave function,[39] and afterward reoptimized in the implicit solvent using the Density Functional Theory (DFT) approach with the GAMESS-US program.[40] In the lowest energy conformer, sulfonamide nitrogen forms a hydrogen bond with the sulfonyl oxygen at the *ortho* position (Figure 9B, bottom). The approximate conformational energy of the docked conformation was also computed using DFT, keeping frozen the sulfonamide S−N and methylsulfonyl S−C bond torsional angles for the benzene ring, and optimizing the rest of the 2-methylsulfonylbenzenesulfonamide molecule (Figure 9B, top). The freezing of the select torsions was necessary because the DFT calculation lacks the protein environment that keeps them at certain values seen in docking. The energy difference between the lowest energy and the docked conformers in Figure 9B was 53.8 kJ/mol. It became clear that the used scoring function did not report a correct binding energy of the conformation in Figure 9A because the Vinardo scoring function neither takes into account the change of the ligand conformation when going from the solution into the receptor, nor the ligand intramolecular energy (in fact, none of the several built-in scoring functions in Smina do). This means that in the conformation shown in Figure 9A the 2-methylsulfonyl group must rotate to avoid the rather severe clash with the sulfonamide oxygens (Figure 9B, top), and by doing so the hydrophobic substituent rotates away from Phe131, potentially yielding other clashes with the protein and leading to the poor binding energies.

Series **7** compounds are more complex to investigate because two enantiomers of the S atom of sulfinyl exist (Figure 9C,D). We will explore the behavior of sulfinyl-containing series **7** using compound **7a** as an example. One of its docked enantiomers, *(S)*-**7a** forms sulfonyl-sulfinyl clash (Figure 9C and the top left part of Figure 9D) similar to what we found for **9a**. The docked *(R)*-**7a** enantiomer is about 1.7 times more stable compared to the *(S)*- enantiomer because of the lack of the clash (Figure 9D,F). Calculations also show that in the absence of the protein,

https://doi.org/10.1021/acs.jmedchem.5c01421
J. Med. Chem. 2025, 68, 17752−17773

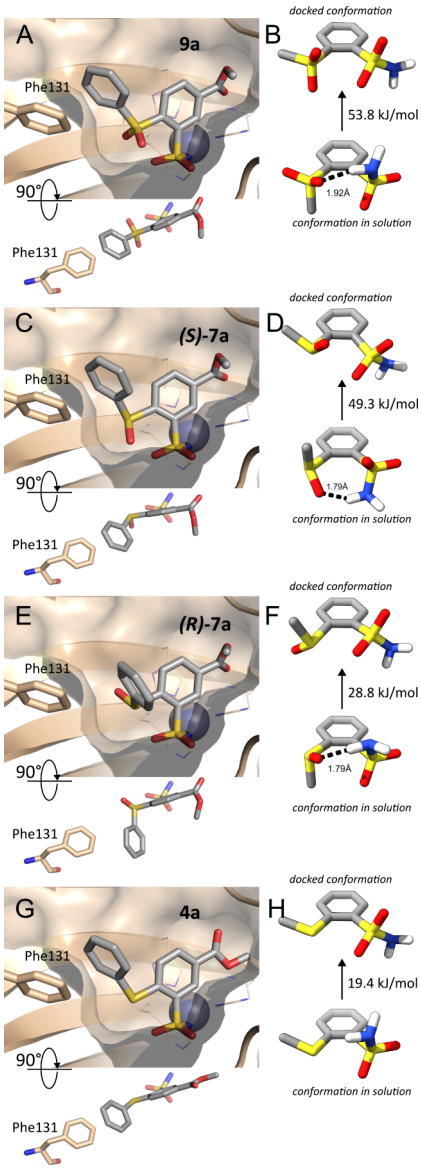

Figure 9. Best ranking docked pose of **9a**, (S)-**7a**, (R)-**7a**, and **4a** in the active site of CAII as a model protein. (A) Best-ranking docked pose of **9a**. While the phenyl substituent stacks well with the Phe131 side chain, the two SO_2 moieties presumably clash. (B) Two conformations of 2-(methylsulfonyl)benzenesulfonamide: Top: conformation with two benzene-to-S bond dihedrals constrained so that it is similar to the docked conformation in (A); bottom: lowest energy conformation with an intramolecular H-bond that is likely to be found in solution. The energy difference between the two rotamers computed using density functional theory is 53.8 kJ/mol. The fact that the used scoring function does not take into account this difference explains why the calculated affinities (not shown) do not match the experimental values. (C), (E) Best-ranked docked conformations of *(S)*- and *(R)*-**7a**, correspondingly. (D), (F) Top: the conformations 2-(methylsulfinyl)-benzenesulfonamide, matching the docked geometries in (C) and (E). Bottom: The lowest energy conformer with an intramolecular H-bond, presumably existing in solution. The docked *(R)*- enantiomer is much more stable due to the lack of clashes present in the docked *(S)*-enantiomer. (G) Best-ranking docked pose of **4a**. (H) Two conformations of 2-methylsulfanylbenzenesulfonamide: Top: the optimized with constraints conformation matching the docked conformation; bottom: The lowest energy conformer. Compared with the sulfinyl- and sulfonyl-forms, the docked conformation for the sulfanyl analog is the most stable, which is also reflected in the binding affinities.

the preferred conformation **7a** (of either chirality) has an intramolecular H-bond (Figure 9D,F, bottom).

For comparison, we also used DFT calculations of the 2-methylsulfanylbenzenesulfonamide molecule to estimate the stability of the docked **4a** (Figure 9G), which does not seem to exhibit clashes. Comparison of Figure 9B,D,F,H shows that the docked conformer **4a** is ∼1.5 times more stable than the most stable docked conformer of **7a** and nearly 3 times more stable than docked **9a**, corresponding to the experimentally determined binding affinities that are best in series **4**, followed by **7** and **9**. Interestingly, calculations suggest that one reason for the relative stability of docked **4** is the lack of the intramolecular hydrogen bond in solution (Figure 9H, bottom), and this observation could be potentially used in designing better binders for carbonic anhydrases, or even other receptors.

■ DISCUSSION

Recognition of the pockets on the protein surface by small-molecule ligands is still rather poorly understood, and it is not possible to accurately calculate the thermodynamic binding parameters.[41] Primary sulfonamide compounds are known to inhibit CA isozymes by binding to the catalytic Zn(II). Chemical variation of the remaining molecule often has a limited influence on binding affinity and selectivity. However, some chemical changes made near the sulfonamide group have a significant impact and may change the behavior from strong binder to completely undetectable binding. To investigate this phenomenon, we synthesized *ortho*-substituted benzenesulfonamides, determined their binding affinity to all catalytically active isoforms of human carbonic anhydrases, obtained crystal structures with CAII, CAIX, and CAXIII, and performed molecular docking. Different oxidation forms of the linker at the *ortho* position were used: −S−, −SO−, and $-SO_2-$. Compounds with −SO− or $-SO_2-$ linker were much weaker binders to any CA isozyme than compounds with the −S− linker. Several reasons could cause this. First, a substituent with a higher oxidation state exhibits a stronger electron-withdrawing effect, thus lowering the pK_a of the amine of the sulfonamide group and causing stronger binding. Second, the linker oxygen atoms may prevent the easier rotation of the ligand molecule bonds and prevent conformational changes needed for the ligand to adapt to the protein surface. Third, the oxygen atoms take additional space, and the steric hindrance could be an essential factor in diminishing the binding affinity.

To test the electron-withdrawing effect, the pK_a values of compounds were determined experimentally. The pK_a of compounds containing −S− linker was almost an entire pH unit higher than compounds with linkers −SO− or $-SO_2-$. Sulfonamides bind to CA in their negatively charged deprotonated form.[42] Therefore, the lowering of sulfonamide pK_a increases the fraction of the binding-ready deprotonated sulfonamide and thus increases the observed affinity. This effect is simply the effect of compound availability in the proper form. To eliminate this misleading increase in affinity, we subtract the fraction effects and calculate the *intrinsic* affinity. The intrinsic dissociation constants of all compounds are provided next to the observed values in the table. In all cases, the intrinsic affinities are higher than the observed ones. The intrinsic values show the 'real' affinities between the binding components in the binding-ready protonation state. These values should be used in drug design to explain the structure−function relationship of the compound effects and not the experimentally observed ones. However, the experimentally observed affinity values show the

https://doi.org/10.1021/acs.jmedchem.5c01421
J. Med. Chem. 2025, 68, 17752−17773

affinities observed by any experimental technique, and the values are biologically relevant. They should be used to calculate the bound fractions and drug effect at particular conditions.

Furthermore, the compounds with a higher oxidation state (**7a, b, h, i, k−m** and **9a−d, h, i, l, m**) did not bind or bind with lower affinity than compounds **4a−d, f−m**. Even the compounds **7h** and **9h** with the smallest methyl substituent did not match the sulfanyl compound **4h** in affinity. The main reason for this was the allowed conformations of the compounds, which were calculated using quantum Density Functional Theory (DFT). The oxygen atoms limited both the flexibility of the molecule in finding the optimal position and acted as a steric hindrance. The present study shows that the *ortho* modifications had a more significant effect than the *para* variations.[21]

The highest affinity for CAIX in this study was exhibited by compound **4b** (methyl 4-cyclohexylsulfanyl-3-sulfamoylbenzoate). Previously we have designed similar compounds bearing 2-chloro or 2-bromo substituents that exhibited slightly higher affinity for CAIX.[20] Here, we have intentionally omitted the halogen atoms to synthesize the *ortho*-substituted compounds more easily and explore the binding without halogens. It was also easier to synthesize compounds with an amide substituent in the *meta* position. The length of these amide-substituted compounds was of limited importance in the previous study but had a significant influence on this study, likely due to reasons of steric hindrance.

Sulfonamide compounds usually bind to CA isozymes by forming a coordination bond between the Zn(II) and sulfonamide amino groups. This bond significantly increases the affinity, but is not necessary for binding to occur.[43] Removal of the metal or change of the metal with another demonstrated that the coordination bond contribution is additive and metal-dependent. Strongly binding compounds like brinzolamide to CAII also bind to the Zn-free apoCAII. The energy contribution of the coordination bond could be determined by using a metal-exchange approach.

In the crystal structure of compound **4h** bound to CAII, two well-resolved compound molecules were bound in the active site. The first was bound in a conventional way forming a coordination bond with the Zn(II), but the second was bound to the protein residues without forming a coordination bond with the Zn(II). This second compound molecule did not bind solely due to crystal-forming effects because it did not bind to the second protein molecule. Therefore, the binding of the second molecule is likely not an artifact. However, the presence of the second molecule in the crystal structure does not mean that it is bound as strongly, nor that we can measure its binding affinity experimentally. Binding assays showed that the stoichiometry here was 1:1, and the affinity of the second molecule was likely weak compared to the first one. Compound concentration in the crystallization experiments was relatively high, millimolar, thus the second molecule could be seen in the crystal structure even if the K_d was in the millimolar range and therefore not interfering in any binding assays. This also means that the second molecule is biologically irrelevant and would not play an essential role in drug design.

■ CONCLUSIONS

The strategy to acidify the pK_a of *ortho* sulfanyl-substituted benzenesulfonamides by oxidation, with the goal of increased affinity to CA, yielded an unexpected drop of affinity in the order of hundreds of thousands of times. Small changes in chemical structures influenced the flexibility of the molecule's substituents and steric restrictions on interactions with proteins. Furthermore, some minor changes led to the discovery of novel CAIX inhibitors with high affinity and selectivity.

■ EXPERIMENTAL SECTION

Organic Synthesis. All starting materials and reagents were commercial products used without further purification. Melting points of the compounds were determined in open capillaries on a Thermo Scientific 9100 Series and are uncorrected. ^{1}H and ^{13}C NMR spectra (Figure S7) were recorded on a (400 and 100 MHz, respectively) spectrometer in DMSO-d_6 using residual DMSO signals (2.52 and 40.21 ppm for ^{1}H and ^{13}C NMR spectra, respectively) as the internal standard. TLC was performed with silica gel 60 F254 aluminum plates (Merck) and visualized with UV light. Column chromatography used silica gel 60 (0.040−0.063 mm, Merck). High-resolution mass spectra (HRMS) were recorded by an Agilent TOF 6230 equipped with an Agilent Infinity 1260 HPLC system (Agilent Technologies). HPLC verified the purity of final compounds to be >95% (Figure S8) using the Agilent Infinity 1260 instrument with a ZORBAX Eclipse Plus C18 Rapid Resolution 4.6 × 100 mm 3.5 μm column, ZORBAX Eclipse Plus-C18 4.6 × 12.5 mm 5.0 μm analytical guard column, eluents A − 20 mM ammonium acetate (pH = 6.9 of unadjusted solution) and B − 100% MeOH was used. HPLC gradient elution with a flow rate of 0.80 mL/min was used, B gradient: 0−10 min 55−95%, 10−14 min 95%. UV detection was recorded at 254 nm. Figure S9 contains ESI-MS spectra of representative compounds.

*Methyl 4-Chloro-3-sulfamoyl-benzoate (**2**).* 4-chloro-3-sulfamoylbenzoic acid **1** (1.78 g, 7.55 mmol, Sigma-Aldrich) was refluxed in MeOH (30 mL) with concentrated H_2SO_4 (0.3 mL) for 8 h. The reaction mixture was concentrated under reduced pressure. Residue was filtered, washed with H_2O and crystallized from H_2O:MeOH(4:1). Yield: 1.70 g, 91%, mp 129−130 °C (Literature[44] mp 124−125 °C).

^{1}H NMR (400 MHz, DMSO-d_6) δ ppm: 3.91 (s, 3H, C**H$_3$**O), 7.80 (d, J = 8.4 Hz, 1H, Ar**H**), 7.84 (s, 2H, SO$_2$N**H$_2$**), 8.14 (dd, J = 8.4 Hz, J = 2.1 Hz, 1H, Ar**H**), 8.52 (d, J = 2.1 Hz, 1H, Ar**H**).

*N-Butyl-4-chloro-3-sulfamoyl-benzamide (**3**).* The mixture of 4-chloro-3-sulfamoylbenzoic acid **1** (500 mg, 2.12 mmol), $SOCl_2$ (0.616 mL, 8.48 mmol), and one drop DMF in toluene (6.0 mL) was refluxed for four h. Excess $SOCl_2$ and toluene were removed by distillation under reduced pressure. The crude acid chloride was dissolved in THF (20 mL) and added dropwise to a solution of *N*-butylamine (0.591 mL, 6.0 mmol) in THF (20 mL) at 0 °C and allowed stirring for one h. The mixture was warmed to room temperature and stirred for another 4 h. THF was removed under reduced pressure. The crude product was crystallized from H_2O. Yield: 492 mg, 80%, mp 172−173 °C (lit.[45] mp 171−172 °C).

^{1}H NMR (400 MHz, DMSO-d_6) δ ppm: 0.92 (t, J = 7.3 Hz, 3H, C**H$_3$**CH$_2$), 1.37 (sextet, J = 7.3 Hz, 2H, C**H$_2$**CH$_3$), 1.54 (quint, J = 7.3 Hz, 2H, CH$_2$**CH$_2$**CH$_2$), 3.29 (q, J = 6.8 Hz, 2H, C**H$_2$**NH), 7.72 (s, 2H, SO$_2$N**H$_2$**), 7.77 (d, J = 8.2 Hz, 1H, Ar**H**), 8.04 (dd, J = 8.2 Hz, J = 2.0 Hz, 1H, Ar**H**), 8.45 (d, J = 2.0 Hz, 1H, Ar**H**), 8.77 (t, J = 5.5 Hz, 1H, N**H**).

*General Procedure for the syntheses of **4a−d, f, g, i−m**.* The mixture of methyl 4-chloro-3-sulfamoylbenzoate **2** (285 mg, 1,14 mmol), DMF (4.0 mL), appropriate thiol (1.25 mmol), and K_2CO_3 (630 mg, 4,56 mmol) was heated at 80 °C for 4−6 h in an inert atmosphere (argon). The mixture was cooled to room temperature, and 10 mL of H_2O was added. The product was extracted with EtOAc (3 × 8 mL). The organic layer was washed with H_2O, dried over anhydrous $MgSO_4$, filtered, and concentrated under reduced pressure.

*Methyl 4-Phenylsulfanyl-3-sulfamoyl-benzoate (**4a**).* The product was purified by flash chromatography on silica gel ($CHCl_3$:EtOAc, 6:1). Yield: 303 mg, 82%, mp 155−156 °C. (lit.[46] mp 154−157).

^{1}H NMR (400 MHz, DMSO-d_6) δ ppm: 3.86 (s, 3H, C**H$_3$**O), 7.00 (d, J = 8.4 Hz, 1H, Ar**H**), 7.55−7.62 (m, 5H, Ar**H**), 7.74 (s, 2H, SO$_2$N**H$_2$**), 7.93 (dd, J = 8.4 Hz, J = 1.9 Hz, 1H, Ar**H**), 8.46 (t, J = 1.9 Hz, 1H, Ar**H**).

https://doi.org/10.1021/acs.jmedchem.5c01421
J. Med. Chem. 2025, 68, 17752−17773

^{13}C NMR (100 MHz, DMSO-d_6) δ ppm: 52.9, 126.8, 129.0, 129.2, 130.5, 130.8, 131.0, 132.6, 135.5, 140.8, 144.2, 165.4.

HRMS calcd for $C_{14}H_{13}NO_4S_2$ [(M+H)$^+$]: 324.0359, found: 324.0354.

*Methyl 4-Cyclohexylsulfanyl-3-sulfamoyl-benzoate (**4b**).* The product was purified by flash chromatography on silica gel ($CHCl_3$:EtOAc, 7:1). Yield: 315 mg, 84%, mp 119−120 °C.

^{1}H NMR (400 MHz, DMSO-d_6) δ ppm: 1.26−1.99 (m, 10H, C**H** cyclohexyl), 3.61 (m, 1H, C**H**S), 3.88 (s, 3H, C**H$_3$**O), 7.47 (s, 2H, SO$_2$N**H$_2$**), 7.74 (d, *J* = 8.4 Hz, 1H, Ar**H**), 8.04 (dd, *J* = 8.3 Hz, *J* = 1.9 Hz, 1H, Ar**H**), 8.43 (d, *J* = 1.9 Hz, 1H, Ar**H**).

^{13}C NMR (100 MHz, DMSO-d_6) δ ppm: 25.7, 25.8, 32.5, 44.4, 52.9, 100.0, 125.9, 129.1, 132.3, 141.7, 142.8, 165.6.

HRMS calcd for $C_{14}H_{19}NO_4S_2$ [(M+H)$^+$]: 330.0828, found: 330.0833.

*Methyl 4-Benzylsulfanyl-3-sulfamoyl-benzoate (**4c**).* The product was purified by flash chromatography on silica gel ($CHCl_3$:EtOAc, 6:1). Yield: 211 mg, 55%, mp 135−136 °C.

^{1}H NMR (400 MHz, DMSO-d_6) δ ppm: 3.88 (s, 3H, C**H$_3$**O), 4.43 (s, 2H, C**H$_2$**S), 7.29−7.37 (m, 3H, Ar**H**), 7.51−7.53 (m, 2H, Ar**H**), 7.58 (s, 2H, SO$_2$N**H$_2$**), 7.74 (d, *J* = 8.3 Hz, 1H, Ar**H**), 8.02 (dt, *J* = 8.3 Hz, *J* = 1.7 Hz, 1H, Ar**H**), 8.42 (t, *J* = 2.2 Hz, 1H, Ar**H**).

^{13}C NMR (100 MHz, DMSO-d_6) δ ppm: 36.4, 52.9, 125.9, 127.7, 128.0, 128.9, 129.0, 129.8, 132.2, 136.0, 140.7, 143.7, 165.6.

HRMS calcd for $C_{15}H_{15}NO_4S_2$ [(M+H)$^+$]: 338.0515, found: 338.0517.

*Methyl 4-(2-Phenylethylsulfanyl)-3-sulfamoyl-benzoate (**4d**).* The product was purified by flash chromatography on silica gel ($CHCl_3$:EtOAc, 5:1). Yield: 332 mg, 83%, mp 146−147 °C.

^{1}H NMR (400 MHz, DMSO-d_6) δ ppm: 2.99 (t, *J* = 7.5 Hz, 2H, C**H$_2$**Ph), 3.41 (t, *J* = 7.5 Hz, 2H, C**H$_2$**S), 3.88 (s, 3H, C**H$_3$**O), 7.23−7.34 (m, 5H, Ar**H**), 7.51 (s, 2H, SO$_2$N**H$_2$**), 7.73 (d, *J* = 8.4 Hz, 1H, Ar**H**), 8.05 (dd, *J* = 8.4 Hz, *J* = 1.8 Hz, 1H, Ar**H**), 8.43 (d, *J* = 1.8 Hz, 1H, Ar**H**).

^{13}C NMR (100 MHz, DMSO-d_6) δ ppm: 33.4, 34.3, 52.9, 125.8, 126.9, 127.8, 128.8, 128.9, 129.1, 132.4, 140.2, 141.,0, 143.6, 165.6.

HRMS calcd for $C_{16}H_{17}NO_4S_2$ [(M+H)$^+$]: 352.0672, found: 352.0675.

*Methyl 4-Cyclododecylsulfanyl-3-sulfamoyl-benzoate (**4f**).* The product was purified by flash chromatography on silica gel ($CHCl_3$:EtOAc, 10:1). Yield: 203 mg, 43%, mp 167−168 °C.

^{1}H NMR (400 MHz, DMSO-d_6) δ ppm: 1.32−1.59 (m, 20H, C**H** cyclododecyl), 1.76 (m, 2H, C**H** cyclododecyl), 3.66 (m, 1H, C**H**S), 3.88 (s, 3H, C**H$_3$**O), 7.47 (s, 2H, SO$_2$N**H$_2$**), 7.70 (d, *J* = 8.4 Hz, 1H, Ar**H**), 8.07 (dd, *J* = 8.4 Hz, *J* = 2.0 Hz, 1H, Ar**H**), 8.44 (d, *J* = 2.0 Hz, 1H, Ar**H**).

^{13}C NMR (100 MHz, DMSO-d_6) δ ppm: 22.0, 23.2, 23.3, 24.0, 24.2, 29.2, 43.5, 52.9, 125.9, 129.0, 129.2, 132.3, 142.0, 143.2, 165.6.

HRMS calcd for $C_{20}H_{31}NO_4S_2$ [(M+H)$^+$]: 414.1767, found: 414.1773.

*Methyl 4-(1-Adamantylsulfanyl)-3-sulfamoyl-benzoate (**4g**).* The product was purified by flash chromatography on silica gel ($CHCl_3$:EtOAc, 10:1). Yield: 173 mg, 40%, mp 189−190 °C.

^{1}H NMR (400 MHz, DMSO-d_6) δ ppm: 1.63 (br s, 6H, C**H** adamantanyl), 1.98 (br s, 6H, C**H** adamantanyl), 2.00 (br s, 3H, C**H** adamantanyl), 3.90 (s, 3H, OC**H$_3$**), 7.40 (s, 2H, SO$_2$N**H$_2$**), 7.87 (d, *J* = 8.0 Hz, 1H, Ar**H**), 8.08 (dd, *J* = 8.0 Hz, *J* = 2.0 Hz, 1H, Ar**H**), 8.53 (d, *J* = 2.0 Hz, 1H, Ar**H**).

^{13}C NMR (100 MHz, DMSO-d_6) δ ppm: 30.1, 35.9, 43.8, 52.2, 53.0, 128.8, 128.9, 131.8, 137.7, 137.9, 147.0, 165.5.

HRMS calcd for $C_{18}H_{23}NO_4S_2$ [(M+H)$^+$]: 382.1141, found: 382.1144.

*Methyl 4-Propylsulfanyl-3-sulfamoyl-benzoate (**4i**).* The product was purified by flash chromatography on silica gel ($CHCl_3$:EtOAc, 5:1). Yield: 202 mg, 61%, mp 111−112 °C.

^{1}H NMR (400 MHz, DMSO-d_6) δ ppm: 1.05 (t, *J* = 7.3 Hz, 3H, C**H$_3$**CH$_2$), 1.71 (quint, *J* = 7.3 Hz, 2H, CH$_3$C**H$_2$**), 3.11 (t, *J* = 7.3 Hz, 2H, C**H$_2$**S), 3.88 (s, 3H, C**H$_3$**O), 7.54 (s, 2H, SO$_2$N**H$_2$**), 7.65 (d, *J* = 8.3 Hz, 1H, Ar**H**), 8.04 (dd, *J* = 8.3 Hz, *J* = 1.9 Hz, 1H, Ar**H**), 8.43 (d, *J* = 1.9 Hz, 1H, Ar**H**).

^{13}C NMR (100 MHz, DMSO-d_6) δ ppm: 13.8, 21.7, 33.9, 52.8, 125.6, 127.5, 128.9, 132.3, 140.9, 144.1, 165.6.

HRMS calcd for $C_{11}H_{15}NO_4S_2$ [(M+H)$^+$]: 290.0515, found: 290.0519.

*Methyl 4-tert-Butylsulfanyl-3-sulfamoyl-benzoate (**4j**).* The product was purified by flash chromatography on silica gel ($CHCl_3$:EtOAc, 5:1). Yield: 214 mg, 62%, mp 124−125 °C.

^{1}H NMR (400 MHz, DMSO-d_6) δ ppm: 1.43 (s, 9H, C**H$_3$**), 3.90 (s, 3H, C**H$_3$**O), 7.43 (s, 2H, SO$_2$N**H$_2$**), 7.91 (d, *J* = 8.2 Hz, 1H, Ar**H**), 8.11 (dd, *J* = 8.2 Hz, *J* = 2.0 Hz, 1H, Ar**H**), 8.52 (d, *J* = 2.0 Hz, 1H, Ar**H**).

^{13}C NMR (100 MHz, DMSO-d_6) δ ppm: 31.6, 49.6, 53.0, 128.4, 128.9, 132.0, 136.2, 140.0, 146.1, 165.5.

HRMS calcd for $C_{12}H_{17}NO_4S_2$ [(M+H)$^+$]: 304.0672, found: 304.0671.

*Methyl 4-Isopentylsulfanyl-3-sulfamoyl-benzoate (**4k**).* The product was purified by flash chromatography on silica gel ($CHCl_3$:EtOAc, 5:1). Yield: 265 mg, 74%, mp 92−93 °C.

^{1}H NMR (400 MHz, DMSO-d_6) δ ppm: 0.94 (d, *J* = 6.6 Hz, 6H, C**H$_3$**), 1.57 (td, *J* = 7.8 Hz, *J* = 6.8 Hz, 2H, C**H$_2$**CH), 1.76 (m, 1H, C**H**), 3.11 (t, *J* = 7.8 Hz, 2H, C**H$_2$**S), 3.88 (s, 3H, C**H$_3$**O), 7.52 (s, 2H, SO$_2$N**H$_2$**), 7.67 (d, *J* = 8.4 Hz, Ar**H**), 8.05 (dd, *J* = 8.4 Hz, *J* = 2.0 Hz, 1H, Ar**H**), 8.42 (d, *J* = 2.0 Hz, 1H, Ar**H**).

^{13}C NMR (100 MHz, DMSO-d_6) δ ppm: 22.6, 27.5, 30.2, 36.9, 52.8, 125.6, 127.5, 128.9, 132.3, 140.9, 144.1, 165.6.

HRMS calcd for $C_{13}H_{19}NO_4S_2$ [(M+H)$^+$]: 318.0828, found: 318.0833.

*Methyl 4-Cyclopentylsulfanyl-3-sulfamoyl-benzoate (**4l**).* The product was purified by flash chromatography on silica gel ($CHCl_3$:EtOAc, 8:1). Yield: 259 mg, 72%, mp 106−107 °C.

^{1}H NMR (400 MHz, DMSO-d_6) δ ppm: 1.55−1.65 (m, 4H, C**H** cyclopentyl), 1.73−1.78 (m, 2H, C**H** cyclopentyl), 2.18−2.23 (m, 2H, C**H** cyclopentyl), 3.84−3.92 (m, 4H, C**H$_3$**O and C**H**S), 7.50 (s, 2H, SO$_2$N**H$_2$**), 7.72 (d, *J* = 8.4 Hz, 1H, Ar**H**), 8,.04 (dd, *J* = 8.4 Hz, *J* = 2.0 Hz, 1H, Ar**H**), 8.42 (d, *J* = 2.0 Hz, 1H, Ar**H**).

^{13}C NMR (100 MHz, DMSO-d_6) δ ppm: 25.1, 33.3, 43.9, 52.8, 125.5, 128.4, 128.9, 132.3, 140.8, 144.7, 165.6.

HRMS calcd for $C_{13}H_{17}NO_4S_2$ [(M+H)$^+$]: 316.0672, found: 316.0677.

*Methyl 4-(1-Naphthylsulfanyl)-3-sulfamoyl-benzoate (**4m**).* The product was purified by flash chromatography on silica gel ($CHCl_3$:EtOAc, 8:1). Yield: 281 mg, 66%, mp 187−188 °C.

^{1}H NMR (400 MHz, DMSO-d_6) δ ppm: 3.83 (s, 3H, C**H$_3$**O), 6.64 (d, *J* = 8.4 Hz, 1H, Ar**H**), 7.54−7.64 (m, 2H, Ar**H**), 7.69 (m, 1H, Ar**H**), 7.74 (dd, *J* = 8.4 Hz, *J* = 2.0 Hz, 1H, Ar**H**), 7.93 (s, 2H, SO$_2$N**H$_2$**), 8.04−8.15 (m, 3H, Ar**H**), 8.22 (d, *J* = 8.3 Hz, 1H, Ar**H**), 8.49 (d, *J* = 2.,0 Hz, 1H, Ar**H**).

^{13}C NMR (100 MHz, DMSO-d_6) δ ppm: 52.9, 125.6, 126.7, 126.9, 127.3, 127.5, 128.4, 128.5, 129.1, 129.6, 132.2, 132.5, 133.8, 134.8, 136.8, 140.4, 143.9, 165.4.

HRMS calcd for $C_{18}H_{15}NO_4S_2$ [(M+H)$^+$]: 374.0515, found: 374.0511.

*Methyl 4-Methylsulfanyl-3-sulfamoyl-benzoate (**4h**).* The mixture of methyl 4-chloro-3-sulfamoylbenzoate **2** (308 mg, 1,23 mmol), DMSO (4.0 mL), sodium methanethiolate (259 mg, 3.69 mmol), and K_2CO_3 (509 mg, 3.69 mmol) was heated at 80 °C temperature for 12 h in inert atmosphere(argon). The mixture was cooled to room temperature and 20 mL brine was added. The product was extracted with EtOAc (3 × 10 mL). The organic layer was washed with H_2O, dried over anhydrous $MgSO_4$, filtered, and concentrated under reduced pressure. The product was crystallized from H_2O:MeOH(4:1). Yield: 203 mg, 64%, mp 157−158 °C.

^{1}H NMR (400 MHz, DMSO-d_6) δ ppm: 2.59 (s, 3H, C**H$_3$**S), 3.89 (s, 3H, C**H$_3$**O), 7.54 (s, 2H, SO$_2$N**H$_2$**), 7.61 (d, *J* = 8.3 Hz, 1H, Ar**H**), 8.07 (dd, *J* = 8.3 Hz, *J* = 1.4 Hz, 1H, Ar**H**), 8.42 (d, *J* = 1.4 Hz, 1H, Ar**H**).

^{13}C NMR (100 MHz, DMSO-d_6) δ ppm: 15.5, 52.9, 125.4, 126.6, 128.8, 132.4, 140.4, 145.1, 165.7.

HRMS calcd for $C_9H_{11}NO_4S_2$ [(M+H)$^+$]: 262.0202, found: 262.0199.

*General Procedure for the Syntheses of **5a−d, f−g, j−m**.* The mixture of *N*-butyl-4-chloro-3-sulfamoyl-benzamide **3** (111 mg, 0.381

https://doi.org/10.1021/acs.jmedchem.5c01421
J. Med. Chem. 2025, 68, 17752−17773

mmol), DMF (4.0 mL), appropriate thiol (0.572 mmol), and K_2CO_3 (210 mg, 1.52 mmol) was heated at 80 °C temperature for 12 h in an inert atmosphere(argon). The mixture was cooled to room temperature and 20 mL H_2O was added. The product was extracted with EtOAc (3 × 8 mL). The organic layer was washed with H_2O, dried over anhydrous $MgSO_4$, filtered, and concentrated under reduced pressure.

*N-Butyl-4-phenylsulfanyl-3-sulfamoyl-benzamide (**5a**).* The product was purified by flash chromatography on silica gel ($CHCl_3$:EtOAc, 1:1). Yield: 71 mg, 51%, mp 109−110 °C.

^{1}H NMR (400 MHz, DMSO-d_6) δ ppm: 0.90 (t, J = 7.3 Hz, 3H, C**H$_3$**), 1.33 (sext, J = 7.3 Hz, 2H, CH_2C**H$_2$**CH_3), 1.52 (quint, J = 7.3 Hz, 2H, CH_2C**H$_2$**CH_2), 3.27 (dt, J = 6.9 Hz, J = 5.7 Hz, 2H, C**H$_2$**NH), 6.99 (d, J = 8.3 Hz, 1H, Ar**H**), 7.51−7.58 (m, 5H, Ar**H**), 7.60 (s, 2H, SO_2N**H$_2$**), 7.82 (dd, J = 8.3 Hz, J = 2.0 Hz, 1H, Ar**H**), 8.38 (d, J = 2.0 Hz, 1H, Ar**H**), 8.59 (t, J = 5.7 Hz, 1H, N**H**).

^{13}C NMR (100 MHz, DMSO-d_6) δ ppm: 14.2, 20.1, 31.6, 39.4, 127.5, 129.6, 129.9, 130.5, 130.6, 132.3, 132.4, 134.9, 140.7, 141.2, 164.9.

HRMS calcd for $C_{17}H_{20}N_2O_3S_2$ [(M+H)$^+$]: 365.0988, found: 365.0985.

*N-Butyl-4-cyclohexylsulfanyl-3-sulfamoyl-benzamide (**5b**).* The product was purified by flash chromatography on silica gel ($CHCl_3$:EtOAc, 1:1). Yield: 70 mg, 50%, mp 114−115 °C.

^{1}H NMR (400 MHz, DMSO-d_6) δ ppm: 0.92 (t, J = 7.3 Hz, 3H, C**H$_3$**), 1.23−1.63 (m, 10H, C**H** cyclohexyl and butyl), 1.72 (m, 2H, C**H** cyclohexyl), 1.90−1.96 (m, 2H, C**H** cyclohexyl), 3.29 (q, J = 6.6 Hz, 2H, C**H$_2$**NH), 3.55−3.60 (m, 1H, C**H**S), 7.34 (s, 2H, SO_2N**H$_2$**), 7.70 (d, J = 8.2 Hz, 1H, Ar**H**), 7.96 (dd, J = 8.2 Hz, J = 1.2 Hz, 1H, Ar**H**), 8.36 (d, J = 1.2 Hz, 1H, Ar**H**), 8.64 (t, J = 5.3 Hz, 1H, N**H**).

^{13}C NMR (100 MHz, DMSO-d_6) δ ppm: 14.2, 20.1, 25.7, 25.8, 31.6, 32.5, 39.4, 44.8, 127.6, 129.7, 130.3, 131.6, 139.0, 142.1, 165.1

HRMS calcd for $C_{17}H_{26}N_2O_3S_2$ [(M+H)$^+$]: 371.1458, found: 371.1463.

*4-Benzylsulfanyl-N-butyl-3-sulfamoyl-benzamide (**5c**).* The product was purified by flash chromatography on silica gel ($CHCl_3$:EtOAc, 1:1). Yield: 65 mg, 45%, mp 185−186 °C.

^{1}H NMR (400 MHz, DMSO-d_6) δ ppm: 0.91 (t, J = 7.2 Hz, 3H, C**H$_3$**), 1.36 (sext, J = 7.2 Hz, 2H, C**H$_2$**CH_3), 1.53 (quint, J = 7.2 Hz, 2H, CH_2C**H$_2$**CH_2), 3.28 (q, J = 6.9 Hz, 2H, C**H$_2$**NH), 4.40 (s, 2H, C**H$_2$**S), 7.29 (t, J = 7.1 Hz, 1H, Ar**H**), 7.36 (t, J = 7.1 Hz, 2H, Ar**H**), 7.44 (s, 2H, SO_2N**H$_2$**), 7.52 (d, J = 7.1 Hz, 2H, Ar**H**), 7.66 (d, J = 8.3 Hz, 1H, Ar**H**), 7.94 (dd, J = 8.3 Hz, J = 1.9 Hz, 1H, Ar**H**), 8.36 (d, J = 1.9 Hz, 1H, Ar**H**), 8.62 (t, J = 5.6 Hz, 1H, N**H**).

^{13}C NMR (100 MHz, DMSO-d_6) δ ppm: 14.2, 20.1, 31.6, 36.5, 39.4, 127.6, 127.7, 127.8, 128.9, 129.7, 130.2, 131.2, 136.5, 140.2, 140.7, 165.0.

HRMS calcd for $C_{18}H_{22}N_2O_3S_2$ [(M+H)$^+$]: 379.1145, found: 379.1140.

*N-Butyl-4-(2-phenylethylsulfanyl)-3-sulfamoyl-benzamide (**5d**).* The product was purified by flash chromatography on silica gel ($CHCl_3$:EtOAc, 1:1). Yield: 95 mg, 63%, mp 116−117 °C.

^{1}H NMR (400 MHz, DMSO-d_6) δ ppm: 0.92 (t, J = 7.3 Hz, 3H, C**H$_3$**), 1.37 (sext, J = 7.3 Hz, 2H, C**H$_2$**CH_3), 1.55 (quint, J = 7.3 Hz, 2H, CH_2C**H$_2$**CH_2), 2.98 (t, J = 7.3 Hz, 2H, C**H$_2$**Ar), 3.28 (q, J = 6.6 Hz, 2H, C**H$_2$**NH), 3.34−3.38 (m, 2H, C**H$_2$**S), 7.25−7.27 (m, 1H, Ar**H**), 7.31−7.33 (m, 4H, Ar**H**), 7.35 (s, 2H, SO_2N**H$_2$**), 7.69 (d, J = 8.3 Hz, 1H, Ar**H**), 7.99 (d, J = 8.3 Hz, 1H, Ar**H**), 8.38 (s, 1H, Ar**H**), 8.65 (t, J = 5.4 Hz, 1H, N**H**).

^{13}C NMR (100 MHz, DMSO-d_6) δ ppm: 14.2, 20.1, 31.6, 33.7, 34.4, 39.4, 126.9, 127.5, 127.9, 128.9, 129.0, 130.4, 131.3, 140.1, 140.3, 141.2, 165.1.

HRMS calcd for $C_{19}H_{24}N_2O_3S_2$ [(M+H)$^+$]: 393.1301, found: 393.1297.

*N-Butyl-4-cyclododecylsulfanyl-3-sulfamoyl-benzamide (**5f**).* The product was purified by flash chromatography on silica gel ($CHCl_3$:EtOAc, 3:1). Yield: 76 mg, 44%, mp 166−168 °C.

^{1}H NMR (400 MHz, DMSO-d_6) δ ppm: 0.93 (t, J = 7.3 Hz, 3H, C**H$_3$**), 1.24−1.59 (m, 24H, C**H$_2$**C**H$_2$**CH_3 and C**H** cyclododecyl), 1.72−1.75 (m, 2H, C**H** cyclododecyl), 3.29 (dt, J = 6.8 Hz, J = 5.6 Hz, 2H, C**H$_2$**NH), 3.68 (s, 1H, C**H**S), 7.33 (s, 2H, SO_2N**H$_2$**), 7.66 (d, J = 8.3 Hz, 1H, Ar**H**), 7.99 (dd, J = 8.3 Hz, J = 2.0 Hz, 1H, Ar**H**), 8.37 (d, J = 2.0 Hz, 1H, Ar**H**), 8.64 (t, J = 5.6 Hz, 1H, N**H**).

^{13}C NMR (100 MHz, DMSO-d_6) δ ppm: 14.2, 20.1, 22.1, 23.4, 23.8, 23.9, 24.2, 29.4, 31.6, 39.4, 43.7, 127.6, 129.5, 130.3, 131.6, 139.7, 142.3, 165.1.

HRMS calcd for $C_{23}H_{38}N_2O_3S_2$ [(M+H)$^+$]: 455.2397, found: 455.2399.

*4-(1-Adamantylsulfanyl)-N-butyl-3-sulfamoyl-benzamide (**5g**).* The product was purified by flash chromatography on silica gel ($CHCl_3$:EtOAc, 1:1). Yield: 64 mg, 40%, mp 187−189 °C.

^{1}H NMR (400 MHz, DMSO-d_6) δ ppm: 0.91 (t, J = 6.8 Hz, 3H, C**H$_3$**), 1.34 (sext, J = 7.2 Hz, 2H, C**H$_2$**CH_3), 1.52 (quint, J = 7.2 Hz, 2H, $NHCH_2$C**H$_2$**), 1.63 (br s, 6H, C**H** adamantanyl), 1.95 (br s, 6H, C**H** adamantanyl), 2.01 (br s, 3H, C**H** adamantanyl), 3.28 (q, J = 6.8 Hz, 2H, NHC**H$_2$**), 7.28 (s, 2H, SO_2N**H$_2$**), 7.78 (d, J = 8.0 Hz, 1H, Ar**H**), 7.98 (dd, J = 8.0 Hz, J = 2.0 Hz, 1H, Ar**H**), 8.44 (d, J = 2.0 Hz, 1H, Ar**H**), 8.71 (t, J = 5.6 Hz, 1H, N**H**).

^{13}C NMR (100 MHz, DMSO-d_6) δ ppm: 14.2, 20.1, 30.1, 31.6, 36.0, 39.5, 43.9, 51.8, 127.4, 129.8, 134.0, 134.5, 138.2, 147.3, 165.2.

HRMS calcd for $C_{21}H_{30}N_2O_3S_2$ [(M+H)$^+$]: 423.1771, found: 423.1777.

*N-Butyl-4-tert-butylsulfanyl-3-sulfamoyl-benzamide (**5j**).* The product was purified by flash chromatography on silica gel ($CHCl_3$:EtOAc, 1:1). Yield: 55 mg, 42%, mp 150−152 °C.

^{1}H NMR (400 MHz, DMSO-d_6) δ ppm: 0.91 (t, J = 7.6 Hz, 3H, C**H$_3$**), 1.30−1.37 (m, 2H, CH_2C**H$_2$**CH_3), 1.41 (s, 9H, C(C**H$_3$**)$_3$), 1.52 (quint, J = 7.2 Hz, 2H, $NHCH_2$C**H$_2$**), 3.28 (q, J = 6.0 Hz, 2H, NHC**H$_2$**), 7.31 (s, 2H, SO_2N**H$_2$**), 7.82 (d, J = 7.6 Hz, 1H, Ar**H**), 7.99 (dd, J = 8.0 Hz, J = 1.6 Hz, 1H, Ar**H**), 8.44 (d, J = 2.0 Hz, 1H, Ar**H**), 8.71 (t, J = 5.8 Hz, 1H, N**H**).

^{13}C NMR (100 MHz, DMSO-d_6) δ ppm: 14.2, 20.1, 31.6, 31.7, 39.5, 49.4, 127.5, 130.1, 134.3, 136.2, 137.0, 146.7, 165.2.

HRMS calcd for $C_{15}H_{24}N_2O_3S_2$ [(M+H)$^+$]: 345.1301, found: 345.1295.

*N-Butyl-4-isopentylsulfanyl-3-sulfamoyl-benzamide (**5k**).* The product was purified by flash chromatography on silica gel ($CHCl_3$:EtOAc, 1:1). Yield: 98 mg, 72%, mp 130−132 °C.

^{1}H NMR (400 MHz, DMSO-d_6) δ ppm: 0.89−0.94 (m, 9H, C**H$_3$**), 1.33 (sext, J = 7.2 Hz, 2H, CH_2C**H$_2$**CH_3), 1.48−1.57 (m, 4H, $NHCH_2$C**H$_2$** and SCH_2C**H$_2$**), 1.75 (hept, J = 7.6 Hz, 1H, C**H**(CH_3)$_2$), 3.09 (t, J = 7.8 Hz, 2H, SC**H$_2$**), 3.30 (q, J = 6.4 Hz, 2H, NHC**H$_2$**), 7.38 (s, 2H, SO_2N**H$_2$**), 7.61 (d, J = 8.4 Hz, 1H, Ar**H**), 7.97 (dd, J = 8.3 Hz, J = 1.6 Hz, 1H, Ar**H**), 8.36 (d, J = 1.7 Hz, 1H, Ar**H**), 8.62 (t, J = 5.3 Hz, 1H, N**H**).

^{13}C NMR (100 MHz, DMSO-d_6) δ ppm: 14.2, 20.1, 22.6, 27.5, 30.4, 31.7, 37.2, 39.4, 127.6(2C), 130.4, 131.1, 140.6, 141.0, 165.1.

HRMS calcd for $C_{16}H_{26}N_2O_3S_2$ [(M+H)$^+$]: 359.1458, found: 359.1464.

*N-Butyl-4-cyclopentylsulfanyl-3-sulfamoyl-benzamide (**5l**).* The product was purified by flash chromatography on silica gel ($CHCl_3$:EtOAc, 1:1). Yield: 84 mg, 62%, mp 122−124 °C.

^{1}H NMR (400 MHz, DMSO-d_6) δ ppm: 0.91 (t, J = 7.2 Hz, 3H, C**H$_3$**), 1.33 (sext, J = 7.2 Hz, 2H, CH_2C**H$_2$**CH_3), 1.48−1.67 (m, 6H, $NHCH_2$C**H$_2$** and C**H** cyclopentyl), 1.71−1.81 (m, 2H, C**H** cyclopentyl), 2.12−2.21 (m, 2H, C**H** cyclopentyl), 3.28 (q, J = 6.4 Hz, 2H, NHC**H$_2$**), 3.92 (quint, J = 6.0 Hz, 1H, SC**H**), 7.36 (s, 2H, SO_2N**H$_2$**), 7.66 (d, J = 8.4 Hz, 1H, Ar**H**), 7.96 (d, J = 7.6 Hz, 1H, Ar**H**), 8.36 (s, 1H, Ar**H**), 8.61 (t, J = 5.2 Hz, 1H, N**H**).

^{13}C NMR (100 MHz, DMSO-d_6) δ ppm: 14.2, 20.1, 25.1, 31.7, 33.3, 39.4, 44.2, 127.6, 128.5, 130.3, 131.0, 141.0, 141.2, 165.1.

HRMS calcd for $C_{16}H_{24}N_2O_3S_2$ [(M+H)$^+$]: 357.1301, found: 357.1307.

*N-Butyl-4-(1-naphthylsulfanyl)-3-sulfamoyl-benzamide (**5m**).* The product was purified by flash chromatography on silica gel ($CHCl_3$:EtOAc, 1:1). Yield: 96 mg, 61%, mp 216−218 °C.

^{1}H NMR (400 MHz, DMSO-d_6) δ ppm: (DMSO−D_6): 0.86 (t, J = 7.6 Hz, 3H, C**H$_3$**), 1.28 (sext, J = 7.6 Hz, 2H, CH_2C**H$_2$**CH_3), 1.45 (quint, J = 7.2 Hz, 2H, $NHCH_2$C**H$_2$**), 3.21 (q, J = 6.8 Hz, 2H, NHC**H$_2$**), 6.57 (d, J = 8.4 Hz, 1H, Ar**H**), 7.53−7.63 (m, 3H, Ar**H** and, naphthyl-**H**), 7.68 (t, J = 8.0 Hz, 1H, naphthyl-**H**), 7.83 (s, 2H,

https://doi.org/10.1021/acs.jmedchem.5c01421
J. Med. Chem. 2025, 68, 17752−17773

SO_2NH_2), 8.03 (d, J = 6.8 Hz, 1H, naphthyl-**H**), 8.08 (d, J = 8.0 Hz, 1H, naphthyl-**H**), 8.15 (d, J = 8.4 Hz, 1H, naphthyl-**H**), 8.19 (d, J = 8.4 Hz, 1H, naphthyl-**H**), 8.41 (d, J = 2.0 Hz, 1H, Ar**H**), 8.50 (t, J = 5.6 Hz, 1H, N**H**).

^{13}C NMR (100 MHz, DMSO-d_6) δ ppm: 14.1, 20.0, 31.6, 39.4, 125.8, 126.9, 127.4, 127.7, 128.1, 128.2(2C), 129.5, 130.4, 131.8, 132.1, 133.7, 134.8, 136.5, 140.4, 140.7, 165.1.

HRMS calcd for $C_{21}H_{22}N_2O_3S_2$ [(M+H)$^+$]: 415.1145, found: 415.1151.

*General Procedure for the Syntheses of **6b, c, e**.* The mixture of *N*-butyl-4-chloro-3-sulfamoyl-benzamide **3** (100 mg, 0.344 mmol) and appropriate amine (2.0 mL) was heated at 130 °C for 24 h in an inert atmosphere. The mixture was cooled to room temperature and 2 N HCl(aq) (5 mL) was added. The product was extracted with EtOAc (3 × 5 mL). The organic layer was washed with H_2O, dried over anhydrous $MgSO_4$, filtered, and concentrated under reduced pressure.

*N-Butyl-4-(cyclohexylamino)-3-sulfamoyl-benzamide (**6b**).* The product was purified by flash chromatography on silica gel ($CHCl_3$:EtOAc, 1:1). Yield: 64 mg, 53%, mp 89−91 °C.

^{1}H NMR (400 MHz, DMSO-d_6) δ ppm: 0.91 (t, J = 7.3 Hz, 3H, C**H$_3$**), 1.23−1.60 (m, 10H, C**H$_2$**C**H$_2$**CH$_3$ and C**H** cyclohexyl), 1.66−1.69 (m, 2H, C**H** cyclohexyl), 1.90−1.93 (m, 2H, C**H** cyclohexyl), 3.25 (dt, J = 6.8 Hz, J = 5.7 Hz, 2H, C**H$_2$**NH), 3.49−3.52 (m, 1H, C**H**NH), 6,17 (d, J = 7.6 Hz, 1H, N**H**-cyclohexyl), 6.84 (d, J = 8.8 Hz, 1H, Ar**H**), 7.43 (s, 2H, SO_2N**H$_2$**), 7.85 (dd, J = 8.8 Hz, J = 2.1 Hz, 1H, Ar**H**), 8.21 (d, J = 2.1 Hz, 1H, Ar**H**), 8.25 (t, J = 5.7 Hz, 1H, N**H**).

^{13}C NMR (100 MHz, DMSO-d_6) δ ppm: 14.2, 20.1, 24.4, 25.8, 31.9, 32.3, 39.2, 50.5, 111.8, 120.9, 124.5, 129.2, 132.3, 146.3, 165.4.

HRMS calcd for $C_{17}H_{27}N_3O_3S$ [(M+H)$^+$]: 354.1846, found: 354.1840.

*4-(Benzylamino)-N-butyl-3-sulfamoyl-benzamide (**6c**).* The product was purified by flash chromatography on silica gel ($CHCl_3$:EtOAc, 1:1). Yield: 40 mg, 32%, mp 132−133 °C.

^{1}H NMR (400 MHz, DMSO-d_6) δ ppm: 0.88 (t, J = 7.2 Hz, 3H, C**H$_3$**), 1.35 (sext, J = 7.2 Hz, 2H, C**H$_2$**CH$_3$), 1.49 (quint, J = 7.2 Hz, 2H, CH$_2$C**H$_2$**CH$_2$), 3.23 (dt, J = 6.8 Hz, J = 5.9 Hz, 2H, C**H$_2$**NH), 4.55 (d, J = 5.8 Hz, 2H, PhC**H$_2$**NH), 6.69 (d, J = 8.8 Hz, 1H, Ar**H**), 6.82 (t, J = 5.8 Hz, 1H, N**H**-benzyl), 7.23−7.39 (m, 5H, Ar**H**), 7.49 (s, 2H, SO_2N**H$_2$**), 7.77 (dd, J = 8.8 Hz, J = 2.0 Hz, 1H, Ar**H**), 8.23 (m, 2H, Ar**H** and N**H**).

^{13}C NMR (100 MHz, DMSO-d_6) δ ppm: 14.2, 20.1, 31.8, 39.2, 46.5, 111.9, 121.5, 125.1, 127.4, 128.9, 128.9, 132.1, 139.2, 146.8, 165.4.

HRMS calcd for $C_{18}H_{23}N_3O_3S$ [(M+H)$^+$]: 362.1533, found: 362.1539.

*N-Butyl-4-(cyclooctylamino)-3-sulfamoyl-benzamide (**6e**).* The product was purified by flash chromatography on silica gel ($CHCl_3$:EtOAc, 1:1). Yield: 55 mg, 42%, brownish oily residue.

^{1}H NMR (400 MHz, DMSO-d_6) δ ppm: 0.91 (t, J = 7.3 Hz, 3H, C**H$_3$**), 1.35 (sext, J = 7.3 Hz, 2H, C**H$_2$**CH$_3$), 1.44−1.73 (m, 14H, C**H** cyclooctyl and CH$_2$C**H$_2$**CH$_2$), 1.81−1.86 (m, 2H, C**H** cyclooctyl), 3.25 (dt, J = 6.9 Hz, J = 5.9 Hz, 2H, C**H$_2$**NH), 3.70−3.73 (m, 1H, C**H**NH cyclooctyl), 6.19 (d, J = 7.6 Hz, 1H, N**H**-cyclooctyl), 6.75 (d, J = 8.8 Hz, 1H, Ar**H**), 7.43 (s, 2H, SO_2N**H$_2$**), 7,.86 (dd, J = 8.8 Hz, J = 2.1 Hz, 1H, Ar**H**), 8.19 (d, J = 2.1 Hz, 1H, Ar**H**), 8.24 (t, J = 5.9 Hz, 1H, N**H**).

^{13}C NMR (100 MHz, DMSO-d_6) δ ppm: 14.2, 20.1, 23.6, 25.5, 27.2, 31.7, 31.9, 39.2, 51.9, 111.9, 120.8, 124.6, 129.3, 132.4, 146.1, 165.5.

HRMS calcd for $C_{19}H_{31}N_3O_3S$ [(M+H)$^+$]: 382.2159, found: 382.2155.

*General Procedure for the Syntheses of **7(a, b, h, i, k−m), 8(a, b, k−m)**.* The mixture of appropriate methyl 4-sulfanilsubstituted-3-sulfamoyl-benzoate (**4a, b, h, i, k−m**) or appropriate *N*-butyl-4-sulfanilsubstituted-3-sulfamoyl-benzamide (**8a, b, k−m**) (0.200 mmol), acetic acid (2.0 mL) and 30% H_2O_2 (0.090 mL, 1.15 mmol) was stirred for 12 h. Then 1% Na_2SO_3(aq) (6.0 mL) was added to the mixture and the product was extracted with EtOAc (3 × 5 mL). The organic layer was washed with H_2O, dried over anhydrous $MgSO_4$, filtered, and concentrated under reduced pressure.

*Methyl 4-(Benzenesulfinyl)-3-sulfamoyl-benzoate (**7a**).* The product was purified by flash chromatography on silica gel ($CHCl_3$:EtOAc, 3:1). Yield: 56 mg, 82%, mp 107−108 °C.

^{1}H NMR (400 MHz, DMSO-d_6) δ ppm: 3,91 (s, 3H, C**H$_3$**O), 7.48−7.53 (m, 3H, Ar**H**), 7.75−7.78 (m, 2H, Ar**H**), 8.09 (s, 2H, SO_2N**H$_2$**), 8.32 (d, J = 8.2 Hz, 1H, Ar**H**), 8.37 (dd, J = 8.2 Hz, J = 1.7 Hz, 1H, Ar**H**), 8.47 (d, J = 1.7 Hz, 1H, Ar**H**).

^{13}C NMR (100 MHz, DMSO-d_6) δ ppm: 53.3, 125.6, 126.9, 128.5, 129.9, 131.6, 132.8, 133.9, 142.3, 145.9, 149.7, 164.9.

HRMS calcd for $C_{14}H_{13}NO_5S_2$ [(M+H)$^+$]: 340.0308, found: 340.0311.

*Methyl 4-Cyclohexylsulfinyl-3-sulfamoyl-benzoate (**7b**).* The product was purified by flash chromatography on silica gel ($CHCl_3$:EtOAc, 3:1). Yield: 52 mg, 75%, mp 188−189 °C.

^{1}H NMR (400 MHz, DMSO-d_6) δ ppm: 1.14−2.07 (m, 10H, C**H$_2$** cyclohexyl), 2.96−3.04 (m, 1H, C**H**SO), 3.94 (s, 3H, C**H$_3$**O), 7.97 (s, 2H, SO_2N**H$_2$**), 8.11 (d, J = 8.2 Hz, 1H, Ar**H**), 8.38 (dd, J = 8.2 Hz, J = 1.7 Hz, 1H, Ar**H**), 8.51 (d, J = 1.7 Hz, 1H, Ar**H**).

^{13}C NMR (100 MHz, DMSO-d_6) δ ppm: 20.9, 25.1, 25.4, 26.1, 28.6, 53.3, 60.9, 127.3, 129.1, 132.5, 132.6, 142.1, 146.5, 165.1.

HRMS calcd for $C_{14}H_{19}NO_5S_2$ [(M+H)$^+$]: 346.0777, found: 346.0783.

*Methyl 4-Methylsulfinyl-3-sulfamoyl-benzoate (**7h**).* The product was purified by flash chromatography on silica gel ($CHCl_3$:EtOAc, 5:1). Yield: 50 mg, 90%, mp 258−259 °C.

^{1}H NMR (400 MHz, DMSO-d_6) δ ppm: 2.81 (s, 3H, C**H$_3$**SO), 3.95 (s, 3H, C**H$_3$**O), 7.97 (s, 2H, SO_2N**H$_2$**), 8.34 (d, J = 8.2 Hz, 1H, Ar**H**), 8.43 (dd, J = 8.2 Hz, J = 1.6 Hz, 1H, Ar**H**), 8.47 (d, J = 1.6 Hz, 1H, Ar**H**).

^{13}C NMR (100 MHz, DMSO-d_6) δ ppm: 44.6, 53.3, 125.7, 128.5, 132.6, 133.8, 141.5, 151.2, 165.1.

HRMS calcd for $C_9H_{11}NO_5S_2$ [(M+H)$^+$]: 278.0151, found: 278.0155.

*Methyl 4-Propylsulfinyl-3-sulfamoyl-benzoate (**7i**).* The product was purified by flash chromatography on silica gel ($CHCl_3$:EtOAc, 3:1). Yield: 40 mg, 66%, mp 144−145 °C.

^{1}H NMR (400 MHz, DMSO-d_6) δ ppm: 0.99 (t, J = 7.4 Hz, 3H, C**H$_3$**CH$_2$), 1.59−1.62 (m, 1H, C**H$_A$**H$_B$CH$_3$); 1,77−1.81 (m, 1H, CH$_A$**H$_B$**CH$_3$), 2.66−2.69 (m, 1H, C**H$_A$**H$_B$SO), 3.10−3.13 (m, 1H, CH$_A$**H$_B$**SO), 3.93 (s, 3H, C**H$_3$**O), 7.97 (s, 2H, SO_2N**H$_2$**), 8.26 (d, J = 8.2 Hz, 1H, Ar**H**), 8.41 (dd, J = 8.2 Hz, J = 1.7 Hz, 1H, Ar**H**), 8.48 (d, J = 1.7 Hz, 1H Ar**H**).

^{13}C NMR (100 MHz, DMSO-d_6) δ ppm: 13.2, 16.5, 53.3, 58.9, 126.3, 128.7, 132.5, 133.4, 141.7, 149.2, 165.1.

HRMS calcd for $C_{11}H_{15}NO_5S_2$ [(M+H)$^+$]: 306.0464, found: 306.0470.

*Methyl 4-Isopentylsulfinyl-3-sulfamoyl-benzoate (**7k**).* The product was purified by flash chromatography on silica gel ($CHCl_3$:EtOAc, 5:1). Yield: 37 mg, 55%, mp 98−99 °C.

^{1}H NMR (400 MHz, DMSO-d_6) δ ppm: 0.86 (d, J = 6.5 Hz, 3H, C**H$_3$**), 0.89 (d, J = 6.5 Hz, 3H, C**H$_3$**), 1.40−1.45 (m, 1H, C**H$_A$**H$_B$CH), 1.63−1.68 (m, 2H, C**H**CH$_3$ and CH$_A$**H$_B$**CH), 2.66−2.69 (m, 1H, C**H$_A$**H$_B$SO), 3.15−3.19 (m, 1H, CH$_A$**H$_B$**SO), 3.94 (s, 3H, C**H$_3$**O), 7.97 (s, 2H, SO_2N**H$_2$**), 8.26 (d, J = 8.2 Hz, 1H, Ar**H**), 8.41 (dd, J = 8.2 Hz, J = 1.7 Hz, 1H, Ar**H**), 8.49 (d, J = 1.7 Hz, 1H, Ar**H**).

^{13}C NMR (100 MHz, DMSO-d_6) δ ppm: 22.4, 22.8, 27.2, 31.4, 53.3, 55.1, 126.4, 128.7, 132.5, 133.4, 141.7, 149.1, 165.1.

HRMS calcd for $C_{13}H_{19}NO_5S_2$ [(M+H)$^+$]: 334.0777, found: 334.0771.

*Methyl 4-Cyclopentylsulfinyl-3-sulfamoyl-benzoate (**7l**).* The product was purified by flash chromatography on silica gel ($CHCl_3$:EtOAc, 4:1). Yield: 51 mg, 77%, mp 109−111 °C.

^{1}H NMR (400 MHz, DMSO-d_6) δ ppm: 1.08−1.18 (m, 1H, C**H** cyclopentyl), 1.43−1.53 (m, 1H, C**H** cyclopentyl), 1.54−1.66 (m, 3H, C**H** cyclopentyl), 1.80−1.94 (m, 2H, C**H** cyclopentyl), 2.00−2.11 (m, 1H, C**H** cyclopentyl), 3.53 (quint, J = 7.6 Hz, 1H, C**H** cyclopentyl), 3.94 (s, 3H, OC**H$_3$**), 7.97 (s, 2H, SO_2N**H$_2$**), 8.16 (d, J = 8.4 Hz, 1H, Ar**H**), 8.36 (dd, J = 8.0 Hz, J = 1.6 Hz, 1H, Ar**H**), 8.49 (d, J = 1.3 Hz, 1H, Ar**H**).

^{13}C NMR (100 MHz, DMSO-d_6) δ ppm: 21.3, 25.7, 26.3, 29.6, 53.3, 61.7, 126.6, 128.9, 132.4, 132.9, 141.7, 148.0, 165.1.

HRMS calcd for $C_{13}H_{17}NO_5S_2$ [(M+H)$^+$]: 332.0621, found: 332.0615.

https://doi.org/10.1021/acs.jmedchem.5c01421
J. Med. Chem. 2025, 68, 17752−17773

*Methyl 4-(1-Naphthylsulfinyl)-3-sulfamoyl-benzoate (**7m**).* The product was purified by flash chromatography on silica gel ($CHCl_3$:EtOAc, 1:1). Yield: 47 mg, 60%, mp 125−127 °C.

^{1}H NMR (400 MHz, DMSO-d_6) δ ppm: 3.93 (s, 3H, C**H**$_3$), 7.61−7.68 (m, 4H, naphthyl-**H**), 8.04−8.08 (m, 1H, naphthyl-**H**), 8.11 (s, 2H, SO_2N**H**$_2$), 8.14 (d, J = 7.6 Hz, 1H, naphthyl-**H**), 8.22 (d, J = 8.0 Hz, 1H, Ar**H**), 8.39 (dd, J = 1.6 Hz, J = 8.0 Hz, 1H, Ar**H**), 8.49−8.52 (m, 1H, naphthyl-**H**), 8.54 (d, 1H, J = 1.6 Hz, Ar**H**).

^{13}C NMR (100 MHz, DMSO-d_6) δ ppm: 53.4, 123.5, 125.5, 126.3, 127.5, 128.0, 128.7, 128.8, 129.2, 129.8, 132.5, 133.2, 133.8 (2C), 141.9, 143.1, 146.7, 165.0.

HRMS calcd for $C_{18}H_{15}NO_5S_2$ [(M+H)$^+$]: 390.0464, found: 390.0460.

*4-(Benzenesulfinyl)-N-butyl-3-sulfamoyl-benzamide (**8a**).* The product was purified by flash chromatography on silica gel ($CHCl_3$:EtOAc, 1:1). Yield: 61 mg, 80%, mp 168−171 °C.

^{1}H NMR (400 MHz, DMSO-d_6) δ ppm: 0.89 (t, J = 7.4 Hz, 3H, C**H**$_3$),), 1.32 (sext, J = 7.8 Hz, 2H, NH(CH$_2$)$_2$C**H**$_2$CH$_3$), 1.50 (quint, J = 7.2 Hz, 2H, NHCH$_2$C**H**$_2$), 3.27 (q, J = 7.2 Hz, 2H, NHC**H**$_2$), 7.47−7.53 (m, 3H, Ar**H**), 7.75 (d, J = 6.4 Hz, 2H, Ar**H**), 7.97 (s, 2H, SO_2N**H**$_2$), 8.20 (s, 2H, Ar**H**), 8.35 (s, 1H, Ar**H**), 8.77 (t, J = 5.4 Hz, 1H, N**H**).

^{13}C NMR (100 MHz, DMSO-d_6) δ ppm: 14.1, 20.1, 31.5, 39.6, 125.5, 126.4, 127.2, 129.8, 131.5, 131.7, 138.0, 142.0, 146.3, 147.3, 164.8.

HRMS calcd for $C_{17}H_{20}N_2O_4S_2$ [(M+H)$^+$]: 381.0937, found: 381.0933.

*N-Butyl-4-cyclohexylsulfinyl-3-sulfamoyl-benzamide (**8b**).* The product was purified by flash chromatography on silica gel ($CHCl_3$:EtOAc, 1:1). Yield: 63 mg, 82%, mp 195−196 °C.

^{1}H NMR (400 MHz, DMSO-d_6) δ ppm: 0.93 (t, J = 7.3 Hz, 3H, C**H**$_3$), 1.07−1.18 (m, 3H, C**H** cyclohexyl), 1.29−1.43 (m, 4H, C**H** cyclohexyl and C**H**$_2$CH$_3$), 1.49−1.60 (m, 4H, C**H** cyclohexyl and CH$_2$C**H**$_2$CH$_2$), 1.71−1.74 (m, 1H, C**H** cyclohexyl), 1.81−1.87 (m, 1H, C**H** cyclohexyl), 2.01−2.05 (m, 1H, C**H** cyclohexyl), 3.01 (tt, J = 12.3 Hz, J = 3.6 Hz, 1H, C**H**SO), 3.24−3.29 (m, 2H, C**H**$_2$NH), 7.84 (s, 2H, SO_2N**H**$_2$), 8.02 (d, J = 8.2 Hz, 1H, Ar**H**), 8.24 (dd, J = 8.2 Hz, J = 1.7 Hz, 1H, Ar**H**), 8.41 (d, J = 1.7 Hz, 1H, Ar**H**), 8.82 (t, J = 5.7 Hz, 1H, N**H**).

^{13}C NMR (100 MHz, DMSO-d_6) δ ppm: 14.2, 20.1, 21.0, 25.1, 25.4, 26.1, 28.5, 31.6, 39.5, 60.9, 126.6, 127.9, 130.3, 137.7, 141.7, 143.8, 164.9.

HRMS calcd for $C_{17}H_{26}N_2O_4S_2$ [(M+H)$^+$]: 387.1407, found: 387.1401.

*N-Butyl-4-isopentylsulfinyl-3-sulfamoyl-benzamide (**8k**).* The product was purified by flash chromatography on silica gel ($CHCl_3$:EtOAc, 1:1). Yield: 55 mg, 74%, mp 121−124 °C.

^{1}H NMR (400 MHz, DMSO-d_6) δ ppm: 0.83 (d, J = 6.4 Hz, 6H, S(CH$_2$)$_2$CH(C**H**$_3$)$_2$), 0.92 (t, J = 7.2 Hz, 3H, NH(CH$_2$)$_3$C**H**$_3$), 1.35 (sext, J = 7.2 Hz, 2H, NHCH$_2$CH$_2$C**H**$_2$), 1.45−1.66 (m, 5H, NHCH$_2$C**H**$_2$, SCH$_2$C**H**$_2$C**H**), 3.31 (q, J = 6.8 Hz, 2H, NH**CH**$_2$), 3.66−3.70 (m, 2H, SC**H**$_2$), 7.33 (s, 2H, SO_2N**H**$_2$), 8.25 (d, J = 8.0 Hz, 1H, Ar**H**), 8.30 (dd, J = 8.0 Hz, J = 1.6 Hz, 1H, Ar**H**), 8.60 (d, J = 1.6 Hz, 1H, Ar**H**), 8.96 (t, J = 5.6 Hz, 1H, N**H**).

^{13}C NMR (100 MHz, DMSO-d_6) δ ppm: 14.2, 20.1, 22.3, 27.0, 30.7, 31.5, 39.6, 53.4, 129.6, 131.5, 133.8, 138.1, 140.4, 143.1, 164.2.

HRMS calcd for $C_{16}H_{26}N_2O_4S_2$ [(M+H)$^+$]: 375.1407, found: 375.1411.

*N-Butyl-4-cyclopentylsulfinyl-3-sulfamoyl-benzamide (**8l**).* The product was purified by flash chromatography on silica gel ($CHCl_3$:EtOAc, 1:1). Yield: 47 mg, 63%, mp 103−107 °C.

^{1}H NMR (400 MHz, DMSO-d_6) δ ppm: 0.92 (t, J = 7.2 Hz, 3H, C**H**$_3$), 1.09−1.17 (m, 1H, C**H** cyclopentyl), 1.35 (sext, J = 7.2 Hz, 2H, NH(CH$_2$)$_2$C**H**$_2$CH$_3$), 1.45−1.63 (m, 6H, NHCH$_2$C**H**$_2$, C**H** cyclopentyl), 1.82−1.94 (m, 2H, C**H** cyclopentyl), 2.01−2.10 (m, 1H, C**H** cyclopentyl), 3.26−3.33 (m, 2H, NHC**H**$_2$), 3.52 (quint, J = 7.6 Hz, 1H, C**H** cyclopentyl), 7.85 (s, 2H, SO_2N**H**$_2$), 8.07 (d, J = 8.4 Hz, 1H, Ar**H**), 8.23 (dd, J = 8.0 Hz, J = 1.6 Hz, 1H, Ar**H**), 8.39 (d, J = 1.6 Hz, 1H, Ar**H**), 8.80 (t, J = 5.6 Hz, 1H, N**H**).

^{13}C NMR (100 MHz, DMSO-d_6) δ ppm: 14.2, 20.1, 21.4, 25.8, 26.3, 29.6, 31.5, 39.6, 61.7, 125.9, 127.7, 130.6, 137.7, 141.3, 145.4, 164.9.

HRMS calcd for $C_{16}H_{24}N_2O_4S_2$ [(M+H)$^+$]: 373.1250, found: 373.1255.

*N-Butyl-4-(1-naphthylsulfinyl)-3-sulfamoyl-benzamide (**8m**).* The product was purified by flash chromatography on silica gel ($CHCl_3$:EtOAc, 1:1). Yield: 28 mg, 33%, mp 232−235 °C.

^{1}H NMR (400 MHz, DMSO-d_6) δ ppm: 0.95 (t, J = 7.2 Hz, 3H, C**H**$_3$), 1.38 (sext, J = 7.2 Hz, 2H, NH(CH$_2$)$_2$C**H**$_2$CH$_3$), 1.56 (quint, J = 7.2 Hz, 2H, NHCH$_2$C**H**$_2$), 3.28−3.37 (m, 2H, NHC**H**$_2$), 7.63−7.73 (m, 4H, naphthyl-**H**), 8.08 (s, 2H, SO_2N**H**$_2$), 8.11−8.13 (m, 2H, naphthyl-**H**, Ar**H**), 8.18−8.22 (m, 1H, naphthyl-**H**), 8.26 (dd, J = 1.6 Hz, J = 8.0 Hz, 1H, Ar**H**), 8.47 (d, 1H, J = 1.6 Hz, Ar**H**), 8.52−8.54 (m, 1H, naphthyl-**H**), 8.86 (t, J = 5.6 Hz, 1H, N**H**).

^{13}C NMR (100 MHz, DMSO-d_6) δ ppm: 14.2, 20.1, 31.5, 39.6, 123.5, 125.3, 126.2, 127.4, 127.5, 128.0, 128.3, 129.2, 129.7, 131.5, 132.3, 133.8, 138.4, 142.0, 142.8, 144.3, 164.8.

HRMS calcd for $C_{21}H_{22}N_2O_4S_2$ [(M+H)$^+$]: 431.1094, found: 431.1088.

*General Procedure for the Syntheses of **9(a−d, h, i, l, m)** and **10(b, k−m)**.* The 30% H_2O_2(aq) (1.08 mmol, 0.110 mL) was added in small portions over 3 h to a solution of appropriate methyl 4-sulfanilsubstituted-3-sulfamoyl-benzoate (**4a−d, h, i, l, m**) or appropriate *N*-butyl-4-sulfanilsubstituted-3-sulfamoyl-benzamide (**10b, k−m**) (0.200 mmol) and acetic acid (2.0 mL) at 70 °C and allowed stirring for 6−8h. The solvent was removed under reduced pressure and the resultant precipitate was filtered, and washed with H_2O.

*Methyl 4-(Benzenesulfonyl)-3-sulfamoyl-benzoate (**9a**).* The product was purified by flash chromatography on silica gel ($CHCl_3$:EtOAc, 5:1). Yield: 57 mg, 80%, mp 212−213 °C.

^{1}H NMR (400 MHz, DMSO-d_6) δ ppm: 3.94 (s, 3H, C**H**$_3$O), 7.55 (s, 2H, SO_2N**H**$_2$), 7.61 (t, J = 7.4 Hz, 2H, Ar**H**), 7.70 (t, J = 7.4 Hz, 1H, Ar**H**), 7.95 (d, J = 7.4 Hz, 2H, Ar**H**), 8.43 (dd, J = 8.2 Hz, J = 1.7 Hz, 1H, Ar**H**), 8.61 (d, J = 8.2 Hz, 1H, Ar**H**), 8,64 (d, J = 1.7 Hz, 1H, Ar**H**).

^{13}C NMR (100 MHz, DMSO-d_6) δ ppm: 53.6, 128.4, 129.6, 130.7, 133.9, 134.3, 134.4, 135.1, 140.6, 141.6, 143.4, 164.5.

HRMS calcd for $C_{14}H_{13}NO_6S_2$ [(M+H)$^+$]: 356.0257, found: 356.0266.

*Methyl 4-Cyclohexylsulfonyl-3-sulfamoyl-benzoate (**9b**).* The product was purified by flash chromatography on silica gel ($CHCl_3$:EtOAc, 5:1). Yield: 61 mg, 85%, mp 155−156 °C.

^{1}H NMR (400 MHz, DMSO-d_6) δ ppm: 1.17−1.81 (m, 10H, C**H**$_2$ cyclohexyl), 3.86−3.91 (m, 1H, C**H**SO$_2$), 3.95 (s, 3H, C**H**$_3$O), 7.42 (s, 2H, SO_2N**H**$_2$), 8.25 (d, J = 8.1 Hz, 1H, Ar**H**), 8.42 (dd, J = 8.1 Hz, J = 1.7 Hz, 1H, Ar**H**), 8.70 (d, J = 1.7 Hz, 1H, Ar**H**).

^{13}C NMR (100 MHz, DMSO-d_6) δ ppm: 24.8, 24.9, 25.1, 53.6, 61.8, 130.9, 133.6, 134.9, 135.2, 138.6, 143.8, 164.6.

HRMS calcd for $C_{14}H_{19}NO_6S_2$ [(M+H)$^+$]: 362.0727, found: 362.0721.

*Methyl 4-Benzylsulfonyl-3-sulfamoyl-benzoate (**9c**).* The product was purified by flash chromatography on silica gel ($CHCl_3$:EtOAc, 5:1). Yield: 66 mg, 89%, mp 189−190 °C.

^{1}H NMR (400 MHz, DMSO-d_6) δ ppm: 3.94 (s, 3H, C**H**$_3$O), 5.03 (s, 2H, C**H**$_2$SO$_2$), 7.19−7.21 (m, 2H, Ar**H**), 7.30−7.34 (m, 3H, Ar**H**), 7.53 (s, 2H, SO_2N**H**$_2$), 7.88 (d, J = 8.0 Hz, 1H, Ar**H**), 8.25 (dd, J = 8.0 Hz, J = 1.8 Hz, 1H, Ar**H**), 8.70 (d, J = 1.8 Hz, Ar**H**).

^{13}C NMR (100 MHz, DMSO-d_6) δ ppm: 53.6, 60.9, 127.9, 129.0, 129.3, 130.6, 131.2, 133.4, 134.5, 135.1, 139.4, 143.7, 164.5.

HRMS calcd for $C_{15}H_{15}NO_6S_2$ [(M+H)$^+$]: 370.0414, found: 370.0419.

*Methyl 4-(2-Phenylethylsulfonyl)-3-sulfamoyl-benzoate (**9d**).* The product was purified by flash chromatography on silica gel ($CHCl_3$:EtOAc, 5:1). Yield: 64 mg, 83%, mp 186−187 °C.

^{1}H NMR (400 MHz, DMSO-d_6) δ ppm: 2.98 (t, J = 8.0 Hz, 2H, C**H**$_2$Ph), 3.94 (s, 3H, C**H**$_3$O), 4.02 (t, J = 8.0 Hz, 2H,C**H**$_2$SO$_2$), 7.18−7.27 (m, 5H, Ar**H**), 7.44 (s, 2H, SO_2N**H**$_2$), 8.30 (d, J = 8.0 Hz, 1H, Ar**H**), 8.40 (d, J = 8.0 Hz, 1H, Ar**H**), 8.67 (s, 1H, Ar**H**).

^{13}C NMR (100 MHz, DMSO-d_6) δ ppm: 28.1, 53.6, 55.9, 127.1, 128.9, 129.0, 130.7, 133.9, 134.3, 135.1, 137.9, 140.0, 143.5, 164.5.

https://doi.org/10.1021/acs.jmedchem.5c01421
J. Med. Chem. 2025, 68, 17752−17773

HRMS calcd for $C_{16}H_{17}NO_6S_2$ [(M+H)$^+$]: 384.0570, found: 384.0578.

*Methyl 4-Methylsulfonyl-3-sulfamoyl-benzoate (**9h**).* The product was purified by flash chromatography on silica gel ($CHCl_3$:EtOAc, 5:1). Yield: 55 mg, 95%, mp 187−188 °C.

^{1}H NMR (400 MHz, DMSO-d_6) δ ppm: 3.51 (s, 3H, C**H$_3$**SO$_2$), 3.96 (s, 3H, C**H$_3$**O), 7.42 (s, 2H, SO$_2$N**H$_2$**), 8.36 (d, J = 8.2 Hz, 1H, Ar**H**), 8.45 (dd, J = 8.2 Hz, J = 1.6 Hz, 1H, Ar**H**), 8.67 (d, J = 1.6 Hz, 1H, Ar**H**).

^{13}C NMR (100 MHz, DMSO-d_6) δ ppm: 44.1, 53.6, 130.5, 133.4, 134.1, 135.1, 141.6, 143.2, 164.6.

HRMS calcd for $C_9H_{11}NO_6S_2$ [(M+H)$^+$]: 294.0101, found: 294.0106.

*Methyl 4-Propylsulfonyl-3-sulfamoyl-benzoate (**9i**).* The product was purified by flash chromatography on silica gel ($CHCl_3$:EtOAc, 5:1). Yield: 57 mg, 88%, mp 169−170 °C.

^{1}H NMR (400 MHz, DMSO-d_6) δ ppm: 0.94 (t, J = 7.4 Hz, 3H, C**H$_3$**CH$_2$), 1.63−1.66 (m, 2H, C**H$_2$**CH$_3$), 3.66 (t, J = 7.7 Hz, 2H, C**H$_2$**SO$_2$), 3.96 (s, 3H, C**H$_3$**O), 7.43 (s, 2H, SO$_2$N**H$_2$**), 8.33 (d, J = 8.1 Hz, 1H, Ar**H**), 8.44 (dd, J = 8.1 Hz, J = 1.6 Hz, 1H, Ar**H**), 8.69 (d, J = 1.6 Hz, 1H, Ar**H**).

^{13}C NMR (100 MHz, DMSO-d_6) δ ppm: 13.1, 16.2, 53.6, 56.7, 130.7, 133.9, 134.2, 135.2, 140.2, 143.5, 164.6.

HRMS calcd for $C_{11}H_{15}NO_6S_2$ [(M+H)$^+$]: 322.0414, found: 322.0422.

*Methyl 4-Cyclopentylsulfonyl-3-sulfamoyl-benzoate (**9l**).* The product was purified by flash chromatography on silica gel ($CHCl_3$:EtOAc, 5:1). Yield: 63 mg, 90%, mp 199−200 °C.

^{1}H NMR (400 MHz, DMSO-d_6) δ ppm: 1.55−1.65 (m, 2H, C**H** cyclopentyl), 1.68−1.76 (m, 2H, C**H** cyclopentyl), 1.77−1.86 (m, 2H, C**H** cyclopentyl), 1.88−1.96 (m, 2H, C**H** cyclopentyl), 3.96 (s, 3H, OC**H$_3$**), 4.44 (quint, J = 7.2 Hz, 1H, C**H** cyclopentyl), 7.41 (s, 2H, SO$_2$N**H$_2$**), 8.34 (d, J = 8.0 Hz, 1H, Ar**H**), 8.42 (dd, J = 8.0 Hz, J = 1.6 Hz, 1H, Ar**H**), 8.70 (d, J = 1.6 Hz, 1H, Ar**H**).

^{13}C NMR (100 MHz, DMSO-d_6) δ ppm: 26.0, 27.0, 53.6, 62.7, 130.9, 133.8, 134.6, 135.1, 139.7, 143.6, 164.6.

HRMS calcd for $C_{13}H_{17}NO_6S_2$ [(M+H)$^+$]: 348.0570, found: 348.0560.

*Methyl 4-(1-Naphthylsulfonyl)-3-sulfamoyl-benzoate (**9m**).* The product was purified by flash chromatography on silica gel ($CHCl_3$:EtOAc, 8:1). Yield: 63 mg, 78%, mp 223−224 °C.

^{1}H NMR (400 MHz, DMSO-d_6) δ ppm: 3.92 (s, 3H, OC**H$_3$**), 7.63−7.67 (m, 4H, naphthyl**H** and SO$_2$N**H$_2$**), 7.74 (t, J = 8.0 Hz, 1H, Ar**H**), 8.12−8.14 (m, 1H, naphthyl**H**), 8.25 (d, J = 8.0 Hz, 1H, Ar**H**), 8.31−8.37 (m, 4H, naphthyl**H**), 8.70 (s, 1H, Ar**H**).

^{13}C NMR (100 MHz, DMSO-d_6) δ ppm: 53.6, 123.9, 125.0, 127.5, 127.8, 129.1, 129.9, 130.8, 131.0, 133.0, 133.8, 134.2, 134.9, 135.2, 135.9, 141.8, 143.5, 164.5.

HRMS calcd for $C_{18}H_{15}NO_6S_2$ [(M+H)$^+$]: 406.0414, found: 406.0423.

*N-Butyl-4-cyclohexylsulfonyl-3-sulfamoyl-benzamide (**10b**).* The product was purified by flash chromatography on silica gel ($CHCl_3$:EtOAc, 3:1). Yield: 68 mg, 84%, mp 155−156 °C.

^{1}H NMR (400 MHz, DMSO-d_6) δ ppm: 0.93 (t, J = 7.3 Hz, 3H, C**H$_3$**), 1.17−1.81 (m, 14H, C**H$_2$**C**H$_2$**CH$_3$ and C**H** cyclohexyl), 3.30−3.32 (m, 2H, C**H$_2$**NH), 3.90−3.93 (m, 1H, C**H**SO$_2$), 7.33 (s, 2H, SO$_2$N**H$_2$**), 8.19 (d, J = 8.1 Hz, 1H, Ar**H**), 8.29 (d, J = 8.1 Hz, 1H, Ar**H**), 8.61 (s, 1H, Ar**H**), 8.96 (t, J = 5.3 Hz, 1H, N**H**).

^{13}C NMR (100 MHz, DMSO-d_6) δ ppm: 14.1, 20.1, 24.9, 24.9, 25.1, 31.5, 39.6, 61.8, 129.8, 131.2, 134.4, 136.5, 140.4, 143.4, 164.2.

HRMS calcd for $C_{17}H_{26}N_2O_5S_2$ [(M+H)$^+$]: 403.1356, found: 403.1351.

*N-Butyl-4-isopentylsulfonyl-3-sulfamoyl-benzamide (**10k**).* The product was purified by flash chromatography on silica gel ($CHCl_3$:EtOAc, 1:1). Yield: 53 mg, 68%, mp 160−162 °C.

^{1}H NMR (400 MHz, DMSO-d_6) δ ppm: 0.83 (d, J = 6.4 Hz, 6H, S(CH$_2$)$_2$CH(C**H$_3$**)$_2$), 0.92 (t, J = 7.6 Hz, 3H, NH(CH$_2$)$_3$C**H$_3$**), 1.35 (sext, J = 7.2 Hz, 2H, NHCH$_2$CH$_2$C**H$_2$**), 1.46−1.66 (m, 5H, NHCH$_2$C**H$_2$**, SCH$_2$C**H$_2$**C**H**), 3.31 (q, J = 6.8 Hz, 2H, NHC**H$_2$**), 3.66−3.70 (m, 2H, SC**H$_2$**), 7.33 (s, 2H, SO$_2$N**H$_2$**), 8.25 (d, J = 8.0 Hz, 1H, Ar**H**), 8.30 (dd, J = 8.0 Hz, J = 1.6 Hz, 1H, Ar**H**), 8.60 (s, 1H, Ar**H**), 8.97 (t, J = 5.2 Hz, 1H, N**H**).

^{13}C NMR (100 MHz, DMSO-d_6) δ ppm: 14.2, 20.1, 22.3, 27.0, 30.7, 31.5, 39.7, 53.4, 129.6, 131.5, 133.8, 138.1, 140.4, 143.1, 164.2.

HRMS calcd for $C_{16}H_{26}N_2O_5S_2$ [(M+H)$^+$]: 391.1356, found: 391.1359.

*N-Butyl-4-cyclopentylsulfonyl-3-sulfamoyl-benzamide (**10l**).* The product was purified by flash chromatography on silica gel ($CHCl_3$:EtOAc, 1:1). Yield: 57 mg, 73%, mp 143−145 °C.

^{1}H NMR (400 MHz, DMSO-d_6) δ ppm: 0.92 (t, J = 7.6 Hz, 3H, CH$_2$C**H$_3$**), 1.35 (sext, J = 7.6 Hz, 2H, CH$_2$C**H$_2$**CH$_3$), 1.54 (quint, J = 7.2 Hz, 2H, NHCH$_2$C**H$_2$**), 1.57−1.65 (m, 2H, C**H** cyclopentyl), 1.68−1.85 (m, 4H, C**H** cyclopentyl), 1.88−1.96 (m, 2H, C**H** cyclopentyl), 3.31 (q, J = 6.8 Hz, 2H, NHC**H$_2$**), 4.44 (quint, J = 7.2 Hz, 1H, SO$_2$C**H** cyclopentyl), 7.32 (br. s, 2H, SO$_2$N**H$_2$**), 8.26−8.31 (m, 2H, Ar**H**), 8.62 (s, 1H, Ar**H**), 8.96 (t, J = 5.6 Hz, 1H, N**H**).

^{13}C NMR (100 MHz, DMSO-d_6) δ ppm: 14.2, 20.1, 26.0, 27.0, 31.5, 39.6, 62.6, 129.7, 131.4, 134.1, 137.7, 140.3, 143.2, 164.2.

HRMS calcd for $C_{16}H_{24}N_2O_5S_2$ [(M+H)$^+$]: 389.1199, found: 389.1205.

*N-Butyl-4-(1-naphthylsulfonyl)-3-sulfamoyl-benzamide (**10m**).* The product was purified by flash chromatography on silica gel ($CHCl_3$:EtOAc, 1:1). Yield: 22 mg, 24%, mp 266−268 °C.

^{1}H NMR (400 MHz, DMSO-d_6) δ ppm: 0.89 (t, J = 7.6 Hz, 3H, CH$_2$C**H$_3$**), 1.32 (sext, J = 7.2 Hz, 2H, CH$_2$C**H$_2$**CH$_3$), 1.51 (quint, J = 7.2 Hz, 2H, NHCH$_2$C**H$_2$**), 3.29 (q, J = 6.4 Hz, 2H, NHC**H$_2$**), 7.52 (s, 2H, SO$_2$N**H$_2$**), 7.62−7.68 (m, 2H, naphthyl**H**), 7.74 (t, J = 8.0 Hz, 1H, naphthyl**H**), 8.13−8.15 (m, 1H, naphthyl**H**), 8.19−8.23 (m, 2H, Ar**H**), 8.30 (d, J = 8.4 Hz, 1H, naphthyl**H**), 8.34−8.39 (m, 2H, naphthyl**H**), 8.60 (d, J = 1.6 Hz, 1H, Ar**H**), 8.92 (t, J = 5.2 Hz, 1H, N**H**).

^{13}C NMR (100 MHz, DMSO-d_6) δ ppm: 14.1, 20.1, 31.4, 39.6, 124.0, 125.0, 127.5, 127.8, 129.0, 129.8, 129.9, 130.7, 131.4, 132.7, 134.2, 135.5, 135.8, 139.8, 140.2, 143.1, 164.3.

HRMS calcd for $C_{21}H_{22}N_2O_5S_2$ [(M+H)$^+$]: 447.1043, found: 447.1048.

Protein Preparation. Recombinant human carbonic anhydrases (CAI, CAII, CAIII, CAIV, CAVA, CAVB, CAVI, CAVII, CAIX, CAXII, CAXIII, CAXIV) were expressed and chromatographically purified according to previously published protocols[47] and were used for FTSA experiments. Proteins (CAII and CAXIII) used for crystallization were additionally purified by affinity chromatography and concentrated. CAIX used for crystallization were expressed and purified according to this protocol.[48] Production of recombinant CAII and the extracellular part of CAIX comprising PG and CA domains (residues 38−391) used in SFA experiments is described in ref 49.

Determination of Observed Binding Parameters. *Fluorescent Thermal Shift Assay (FTSA).* Dissociation constants, $K_{d,obs}$, (listed in Table 1) of the compounds binding to CAs were determined by the fluorescent thermal shift assay using a QIAGEN's real-time PCR cycler the "Rotor-Gene Q" and Rotor-Gene Style 4-strip tubes from STARLAB. Ligands were dissolved in DMSO stock solutions to concentrations of 10 mM or 20 mM and used for the serial dilution of the dilution factor 2 in DMSO. These samples were diluted with buffer solution and mixed with a prepared protein solution, consisting of protein stock, buffer solution, and solvatochromic dye 8-anilino-1-naphthalenesulfonate (ANS). All final samples typically contained up to 10 μM CA, compound solutions of serial dilution from 0 μM to 200 μM at 8 different concentrations differing by 2 times, 50 μM ANS, 50 mM sodium phosphate buffer at pH 7.0, 100 mM sodium chloride, and 2.0% (v/v) DMSO. Samples preparation is explained in detail in.[50] The excitation and emission wavelengths of ANS were 365 ± 20 and 460 ± 15 nm. Samples were heated from 25 to 99 °C at the rate of 1 °C/min. The curve-fitting procedure was performed by Thermott[51] at 37 °C. Data are deposited in the public database: Protein−Ligand Binding Database[52] (Database URL: https://plbd.org/).

Stopped-Flow Carbon Dioxide Hydration Assay. Recombinant CAII and the extracellular part of CAIX comprising PG and CA domains (residues 38−391) were used in inhibition assays. A stopped-flow instrument (BioLogic) was used for measuring the CA-catalyzed CO_2 hydration activity in the presence of inhibitors.[53] The assay buffer

https://doi.org/10.1021/acs.jmedchem.5c01421
J. Med. Chem. 2025, 68, 17752−17773

Table 4. Crystallization Conditions Used to Grow Protein Crystals in This Study

PDB ID	isozyme—compound	cystallization buffer	sitting drop
9FPT	CAII—**2**	0.1 M sodium bicine (pH 9.0) and 2 M sodium malonate (pH 7.0)	2 μL of 41 mg/mL CAII solution and 2 μL of crystallization buffer
9FPU	CAII—**3**	0.1 M sodium bicine (pH 9.0) and 2 M sodium malonate (pH 7.0)	2 μL of 41 mg/mL CAII solution and 2 μL of crystallization buffer
9FPQ	CAII—**4c**	0.1 M sodium bicine (pH 9.0), 0.2 M ammonium sulfate, and 2 M sodium malonate (pH 7.0)	2 μL of 41 mg/mL CAII solution and 2.5 μL of crystallization buffer
9FPR	CAII—**4d**	0.1 M sodium bicine (pH 9.0), 0.2 M ammonium sulfate, and 2 M sodium malonate (pH 7.0)	3 μL of 12 mg/mL CAII solution and 3 μL of crystallization buffer
9FPS	CAII—**4h**	0.1 M sodium bicine (pH 9.0) and 2 M sodium malonate (pH 7.0)	3 μL of 12 mg/mL CAII solution and 3 μL of crystallization buffer
9R8X	CAIX—**4d**	1.0 M diammonium hydrogen phosphate and 0.1 M sodium acetate (pH 4.5)	10 mg/mL CAIX solution
9R8Y	CAIX—**5b**	1.0 M diammonium hydrogen phosphate and 0.1 M sodium acetate (pH 4.5)	10 mg/mL CAIX solution
9FPV	CAXIII—**4c**	0.1 M sodium citrate (pH 5.5), 0.1 M sodium acetate (pH 4.5), and 26% of PEG4000	1 μL of 23 mg/mL CAXIII solution and 0.4 μL of crystallization buffer
9FPW	CAXIII—**4d**	0.1 M sodium citrate (pH 5.5), 0.1 M sodium acetate (pH 4.5), and 26% of PEG4000	1 μL of 23 mg/mL CAXIII solution and 0.4 μL of crystallization buffer

consisted of 0.2 mM Phenol Red (pH indicator used in absorbance maximum of 557 nm), 20 mM HEPES Na (pH 7.5), and 20 mM Na_2SO_4. The concentration of CAII and CAIX in the enzyme assay was 4 nM and 1 nM, respectively. To stabilize CAIX during the measurements, 0.0025% dodecyl-β-D-maltopyranoside (DDM, Anatrace, and Anagrade purity) was included in the reaction mixture.

The substrate (CO_2) concentration in the reaction was 8.5 mM. Rates of the CA-catalyzed CO_2 hydration reaction were followed for 30 s at 25 °C. Four traces of substrate conversion in the reaction were fitted by the exponential function to determine the rate for each inhibitor concentration. The uncatalyzed rates were determined in the same manner and subtracted from the total observed rates. Stock solutions of inhibitors (100 mM) were prepared in dimethyl sulfoxide, and dilutions of up to 100 nM were made thereafter in DMSO. Apparent K_i' values were obtained from dose−response curves recorded for at least six different concentrations of the test compound by the nonlinear least-squares method using an Excel spreadsheet fitting the Williams-Morrison equation.[54] K_i values were then derived using the Cheng-Prusoff equation.[55] The K_m values used in the Cheng−Prusoff equation were 9.3 mM for CAII and 7.5 mM for CAIX. Inhibition data are provided in Figure S2.

Calculation of the Intrinsic Binding Parameters. The detailed description of the importance and calculation of the intrinsic values have been previously described.[27] For the calculation of the *intrinsic* dissociation constants, the experimentally measured *observed* dissociation constants determined by the FTSA, the pK_a of the sulfonamide group of the compound, and the pK_a of the water molecule bound to the zinc cation by the CA were used.

The intrinsic dissociation constant, $K_{d,int}$, is equal to

$$K_{d,int} = K_{d,obs} \times f_{RSO_2NH^-} \times f_{CAZnH_2O} \quad (1)$$

The fraction of deprotonated sulfonamide:

$$f_{RSO_2NH^-} = \frac{10^{pH-pK_{a,SA}}}{1 + 10^{pH-pK_{a,SA}}} \quad (2)$$

The fraction of Zn(II)-bound water form of CA:

$$f_{CAZnH_2O} = \frac{10^{pK_{a,CA}-pH}}{1 + 10^{pK_{a,CA}-pH}} \quad (3)$$

- $K_{d,obs}$ − observed dissociation constant;
- $f_{RSO_2NH^-}$ and f_{CAZnH_2O} − fractions of deprotonated sulfonamide and Zn(II)-bound water molecule;
- p$K_{a,SA}$ − pK_a of the sulfonamide group;
- p$K_{a,CA}$ − pK_a value of water molecule bound to Zn(II) in the active site of CA.

In this study, the pH value was equal to 7.0.

Determination of pK_a Values of the Compound Sulfonamide Group. The pK_a values of the water molecule bound to Zn^{2+} in the active site of CAs, p$K_{a,CA}$, were taken from ref 42 and of compounds, p$K_{a,SA}$, (Figure S3) were experimentally determined as described in ref 56.

We used a constant concentration of sulfonamide (25−400 μM) and 2.0% (v/v) or 20% (v/v; but only for very poorly soluble ones) of DMSO in universal buffer (50 mM sodium acetate, 25 mM sodium borate, and 50 mM sodium phosphate) at different pH values (in the range from pH 6.0 to 12.0 with 0.5 pH increment). UV/vis spectra of the compound solution were recorded at 37 °C using BMG Labtech CLARIOstarPlus plate reading spectrophotometer. The pK_a values were calculated by normalizing the absorbance and plotting it as a function of pH, then fitting it to the Henderson−Hasselbalch equation using the least-square method. The midpoint of this fitted curve is equal to the sulfonamide group p$K_{a,SA}$.

X-ray Crystallography. *Crystallization.* Crystals of CAII, CAIX, and CAXIII were obtained using the sitting-drop vapor diffusion method at room temperature. Table 4 lists the concentrations of proteins and buffers used for crystallization.

Ligand Soaking. The crystal structures of CAII and CAXIII with ligands were obtained by soaking. A 50 mM solution of each ligand was prepared in dimethyl sulfoxide. One μL of this solution was then diluted using 50 μL of matching reservoir solution corresponding to the conditions under which the crystal was formed. Crystals were incubated for up to 1 week in the soaking solution.

Cocrystallization. The crystal structures of CAIX with ligands were obtained by cocrystallization. Table 4 lists crystallization conditions. The ligand used for cocrystallization was in 5−10 mM concentration, while the stock solution contained 100 mM ligand dissolved in dimethyl sulfoxide.

Data Collection and Structure Determination. Data for CAII and CAXII were collected at PETRA III BEAMLINE P13 (MX1) and for CAIX at BESSY II beamline 14.1.

The data were processed and scaled using XDS,[58] MOSFLM,[59,60] and SCALA.[61] The crystal structures were solved by molecular replacement using MOLREP.[62] The initial model for molecular replacement−CAII: 3HLJ; CAIX: 8Q18,[63] CAXIII: 2NNO. The structure was refined by REFMAC[64] and remodeled using COOT.[57] The 3D models of compounds were constructed by the AVOGADRO[65] program and ligand parameter files were created using LIBCHECK.[66,67]

The data diffraction and final model refinement statistics and PDB IDs are summarized in Table 3. All graphics were created using PyMOL Molecular Graphics System. Authors will release the atomic coordinates upon article publication.

Molecular Docking. The following receptors PDB IDs were chosen for docking: CAII: 3HS4; CAIX: 6G9U, chain A; CAXIII: 4KNN, chain A. The receptors selected from the Protein Data Bank

https://doi.org/10.1021/acs.jmedchem.5c01421
J. Med. Chem. 2025, 68, 17752−17773

differed from the new X-ray structures presented in this Paper to decrease bias. The proteins were prepared for docking using ChimeraX (version 1.9).[68−70] The ligands were optimized using the MMFF94s force field[71−76] within Avogadro molecular viewer (version 1.2.0).[65] For series **7** ligands, two enantiomers of the chiral sulfur were created and docked separately. The format conversions were performed using OpenBabel (The Open Babel Package, version 3.1.1, http://openbabel.org).[77] The docking was performed using the Smina program (version master:dc3dfab+).[34] Smina is based on Autodock Vina.[36] The constrained optimization was done using Smina, using a custom scoring function with a quadratic bias function with weight $w=-10$ added to the default Vina scoring function.[36] The quadratic constraint forced sulfonamide nitrogen to adhere to its position in the X-ray structure. A cubic docking box of size (24 Å),[3] exhaustiveness 100, and energy range 10 kcal/mol was set as docking parameters. The resulting poses were rescored with Smina using the Vinardo scoring function[38] without the constraint. Only one of the symmetry equivalent poses (e.g., phenyl ring flip) was included when evaluating pose ranking after docking. Heavy atom Root Mean Square Deviations (RMSD) were calculated using DockRMSD software (version 1.1).[78]

The quantum Density Functional Theory (DFT) optimizations were performed using GAMESS-US (version 2019.R2)[40] using DFT functional ωB97X-D[79] with the cc-pVDZ basis set[80,81] and the C-PCM implicit solvation model for water.[82] The conformational search was performed using CREST software (version 3.0.2)[38] using xTB (version 6.7.1)[83] computational engine, employing the GFN2-xTB semiempirical tight binding method[39] and the ALPB implicit solvation model for water.[84]

■ ASSOCIATED CONTENT

Supporting Information

The Supporting Information is available free of charge at https://pubs.acs.org/doi/10.1021/acs.jmedchem.5c01421.

FTSA data of compound binding to CA isozymes; SFA data of CA isozyme inhibition by compounds; determination of pK_a values of compound − RSO_2NH_2; NMR spectra of compounds; HPLC chromatograms of representative compounds; ESI-MS spectra of representative compounds; and comparison of docking and crystallographic binding poses (PDF)

SMILE strings of the synthesized compound and corresponding biological activity: *observed* and *intrinsic* ($K_{d,obs}$ and $K_{d,int}$) dissociation constants (in nM units) of investigated compounds to all catalytically active human CAs at 37 °C obtained by FTSA (CSV)

■ AUTHOR INFORMATION

Corresponding Author

Daumantas Matulis − *Department of Biothermodynamics and Drug Design, Institute of Biotechnology, Life Sciences Center, Vilnius University, Vilnius LT-10257, Lithuania;* orcid.org/0000-0002-6178-6276; Email: daumantas.matulis@bti.vu.lt

Authors

Audrius Zakšauskas − *Department of Biothermodynamics and Drug Design, Institute of Biotechnology, Life Sciences Center, Vilnius University, Vilnius LT-10257, Lithuania*

Vaida Paketurytė-Latvė − *Department of Biothermodynamics and Drug Design, Institute of Biotechnology, Life Sciences Center, Vilnius University, Vilnius LT-10257, Lithuania;* orcid.org/0000-0003-0919-7826

Alberta Jankūnaitė − *Department of Biothermodynamics and Drug Design, Institute of Biotechnology, Life Sciences Center, Vilnius University, Vilnius LT-10257, Lithuania*

Edita Čapkauskaitė − *Department of Biothermodynamics and Drug Design, Institute of Biotechnology, Life Sciences Center, Vilnius University, Vilnius LT-10257, Lithuania*

Yann Becart − *Department of Biothermodynamics and Drug Design, Institute of Biotechnology, Life Sciences Center, Vilnius University, Vilnius LT-10257, Lithuania*

Alexey Smirnov − *Department of Biothermodynamics and Drug Design, Institute of Biotechnology, Life Sciences Center, Vilnius University, Vilnius LT-10257, Lithuania*

Klára Pospíšilová − *Institute of Organic Chemistry and Biochemistry of the Czech Academy of Sciences, Prague 6 16610, Czech Republic*

Janis Leitans − *Latvian Biomedical Research and Study Centre, Riga LV-1067, Latvia*

Jiří Brynda − *Institute of Organic Chemistry and Biochemistry of the Czech Academy of Sciences, Prague 6 16610, Czech Republic*

Andris Kazaks − *Latvian Biomedical Research and Study Centre, Riga LV-1067, Latvia*

Lina Baranauskienė − *Department of Biothermodynamics and Drug Design, Institute of Biotechnology, Life Sciences Center, Vilnius University, Vilnius LT-10257, Lithuania;* orcid.org/0000-0002-9924-9177

Elena Manakova − *Department of Protein−DNA Interactions, Institute of Biotechnology, Life Sciences Center, Vilnius University, Vilnius LT-10257, Lithuania*

Saulius Gražulis − *Sector of Crystallography and Cheminformatics, Institute of Biotechnology, Life Sciences Center, Vilnius University, Vilnius LT-10257, Lithuania*

Visvaldas Kairys − *Department of Bioinformatics, Institute of Biotechnology, Life Sciences Center, Vilnius University, Vilnius LT-10257, Lithuania;* orcid.org/0000-0002-5427-0175

Kaspars Tars − *Latvian Biomedical Research and Study Centre, Riga LV-1067, Latvia;* orcid.org/0000-0001-8421-9023

Pavlína Řezáčová − *Institute of Organic Chemistry and Biochemistry of the Czech Academy of Sciences, Prague 6 16610, Czech Republic*

Complete contact information is available at: https://pubs.acs.org/10.1021/acs.jmedchem.5c01421

Author Contributions

A.Z. and V.P.-L. contributed equally to this paper.

Notes

The authors declare the following competing financial interest(s): Authors declare that they have patents and patent applications pending on CA inhibitors.

■ ACKNOWLEDGMENTS

This research was supported by (i) a grant from the Research Council of Lithuania (No. S-MIP-22-35); (ii) the National Institute for Cancer Research (Programme EXCELES, ID Project No. LX22NPO5102), Funded by the European Union, Next Generation EU awarded to PR; and (iii) the European Union's Recovery and Resilience Mechanism project (No.5.2.1.1.i.0/2/24/I/CFLA/001) "Consolidation of the Latvian Institute of Organic Synthesis and the Latvian Biomedical Research and Study Centre". The authors also thank Martynas Malikėnas for performing HPLC analysis of compounds. We thank Vilma Michailovienė†, who died in 2022, for performing numerous protein affinity purification procedures.

ABBREVIATIONS

CA, human carbonic anhydrase; FTSA, fluorescent thermal shift assay (or differential scanning fluorimetry DSF); int, intrinsic; $K_{d,int}$, intrinsic equilibrium dissociation constant; $K_{d,obs}$, observed equilibrium dissociation constant; obs, observed; $pK_{a,CA}$, pK_a value of water molecule bound to Zn(II) in the active site of CA; $pK_{a,SA}$, pK_a of the sulfonamide group; SFA, stopped-flow carbon dioxide hydration assay

REFERENCES

(1) Whitesides, G. M.; Krishnamurthy, V. M. Designing ligands to bind proteins. *Q. Rev. Biophys.* **2005**, *38*, 385−395.

(2) Maren, T. H. Use of inhibitors in physiological studies of carbonic anhydrase. *Am. J. Physiol.-Ren. Physiol.* **1977**, *232*, F291−F297.

(3) Meldrum, N. U.; Roughton, F. J. Some properties of carbonic anhydrase, the CO2 enzyme present in blood. *J. Physiol* **1932**, *75*, 15P−16P.

(4) *The Carbonic Anhydrases*; Springer US: Boston, MA, 1991.

(5) *The Carbonic Anhydrases*; Birkhäuser Basel: Basel, 2000.

(6) Krishnamurthy, V. M.; et al. Carbonic Anhydrase as a Model for Biophysical and Physical-Organic Studies of Proteins and Protein−Ligand Binding. *Chem. Rev.* **2008**, *108*, 946−1051.

(7) *The Carbonic Anhydrases: Current and Emerging Therapeutic Targets*; Springer International Publishing: Cham, 2021; Vol. 75.

(8) Zamanova, S.; Shabana, A. M.; Mondal, U. K.; Ilies, M. A. Carbonic anhydrases as disease markers. *Expert Opin. Ther. Pat.* **2019**, *29*, 509−533.

(9) *Carbonic Anhydrase: Mechanism, Regulation, Links to Disease, and Industrial Applications*; Springer: Netherlands, Dordrecht, 2014; Vol. 75.

(10) Abbate, F.; et al. Nonaromatic sulfonamide group as an ideal anchor for potent human carbonic anhydrase inhibitors: role of hydrogen-bonding networks in ligand binding and drug design. *J. Med. Chem.* **2002**, *45*, 3583−3587.

(11) Martin, D. P.; Hann, Z. S.; Cohen, S. M. Metalloprotein−Inhibitor Binding: Human Carbonic Anhydrase II as a Model for Probing Metal−Ligand Interactions in a Metalloprotein Active Site. *Inorg. Chem.* **2013**, *52*, 12207−12215.

(12) Carta, F.; Supuran, C. T.; Scozzafava, A. Sulfonamides and their isosters as carbonic anhydrase inhibitors. *Future Med. Chem.* **2014**, *6*, 1149−1165.

(13) Fox, J. M.; Zhao, M.; Fink, M. J.; Kang, K.; Whitesides, G. M. The Molecular Origin of Enthalpy/Entropy Compensation in Biomolecular Recognition. *Annu. Rev. Biophys.* **2018**, *47*, 223−250.

(14) Aggarwal, M.; Boone, C. D.; Kondeti, B.; McKenna, R. Structural annotation of human carbonic anhydrases. *J. Enzyme Inhib Med. Chem.* **2013**, *28*, 267−277.

(15) Supuran, C. T. Structure and function of carbonic anhydrases. *Biochem. J.* **2016**, *473*, 2023−2032.

(16) Lomelino, C. L.; Andring, J. T.; McKenna, R. Crystallography and Its Impact on Carbonic Anhydrase Research. *Int. J. Med. Chem.* **2018**, *2018*, No. 9419521.

(17) Smirnovienė, J.; et al. Switching the Inhibitor-Enzyme Recognition Profile via Chimeric Carbonic Anhydrase XII. *ChemistryOpen* **2021**, *10*, 567−580.

(18) Scott, A. D.; et al. Thermodynamic Optimisation in Drug Discovery: A Case Study using Carbonic Anhydrase Inhibitors. *ChemMedChem.* **2009**, *4*, 1985−1989.

(19) Glöckner, S.; Ngo, K.; Wagner, B.; Heine, A.; Klebe, G. The Influence of Varying Fluorination Patterns on the Thermodynamics and Kinetics of Benzenesulfonamide Binding to Human Carbonic Anhydrase II. *Biomolecules* **2020**, *10*, 509.

(20) Zakšauskas, A.; et al. Methyl 2-Halo-4-Substituted-5-Sulfamoyl-Benzoates as High Affinity and Selective Inhibitors of Carbonic Anhydrase IX. *Int. J. Mol. Sci.* **2021**, *23*, 130.

(21) Zakšauskas, A.; et al. Design of two-tail compounds with rotationally fixed benzenesulfonamide ring as inhibitors of carbonic anhydrases. *Eur. J. Med. Chem.* **2018**, *156*, 61−78.

(22) Zakšauskas, A.; et al. Halogenated and di-substituted benzenesulfonamides as selective inhibitors of carbonic anhydrase isoforms. *Eur. J. Med. Chem.* **2020**, *185*, No. 111825.

(23) MERCAPTANS FROM THIOKETALS: CYCLODODECYL MERCAPTAN. *Org. Synth. 61*, 74 (**1983**).

(24) Mahalingam, S. M.; Chu, H.; Liu, X.; Leamon, C. P.; Low, P. S. Carbonic Anhydrase IX-Targeted Near-Infrared Dye for Fluorescence Imaging of Hypoxic Tumors. *Bioconjugate Chem.* **2018**, *29*, 3320−3331.

(25) Smirnovienė, J.; Smirnovas, V.; Matulis, D. Picomolar inhibitors of carbonic anhydrase: Importance of inhibition and binding assays. *Anal. Biochem.* **2017**, *522*, 61−72.

(26) Taylor, P. W.; King, R. W.; Burgen, A. S. V. Influence of pH on the kinetics of complex formation between aromatic sulfonamides and human carbonic anhydrase. *Biochemistry* **1970**, *9*, 3894−3902.

(27) Zubrienė, A.; Matulis, D. Observed Versus Intrinsic Thermodynamics of Inhibitor Binding to Carbonic Anhydrases. In *Carbonic Anhydrase as Drug Target: Thermodynamics and Structure of Inhibitor Binding*; Matulis, D., Ed.; Springer International Publishing: Cham, 2019; pp 107−123.

(28) Fisher, S. Z.; Aggarwal, M.; Kovalevsky, A. Y.; Silverman, D. N.; McKenna, R. Neutron Diffraction of Acetazolamide-Bound Human Carbonic Anhydrase II Reveals Atomic Details of Drug Binding. *J. Am. Chem. Soc.* **2012**, *134*, 14726−14729.

(29) Aggarwal, M.; et al. Neutron structure of human carbonic anhydrase II in complex with methazolamide: mapping the solvent and hydrogen-bonding patterns of an effective clinical drug. *IUCrJ.* **2016**, *3*, 319−325.

(30) Zubrienė, A.; et al. Intrinsic thermodynamics of 4-substituted-2,3,5,6-tetrafluorobenzenesulfonamide binding to carbonic anhydrases by isothermal titration calorimetry. *Biophys Chem.* **2015**, *205*, 51−65.

(31) Dudutienė, V.; et al. Isoform-Selective Enzyme Inhibitors by Exploring Pocket Size According to the Lock-and-Key Principle. *Biophys. J.* **2020**, *119*, 1513−1524.

(32) Eisenberg, D.; Schwarz, E.; Komaromy, M.; Wall, R. Analysis of membrane and surface protein sequences with the hydrophobic moment plot. *J. Mol. Biol.* **1984**, *179*, 125−142.

(33) Supuran, C. T. How many carbonic anhydrase inhibition mechanisms exist? *J. Enzyme Inhib. Med. Chem.* **2016**, *31*, 345−360.

(34) Koes, D. R.; Baumgartner, M. P.; Camacho, C. J. Lessons Learned in Empirical Scoring with smina from the CSAR 2011 Benchmarking Exercise. *J. Chem. Inf. Model.* **2013**, *53*, 1893−1904.

(35) Quiroga, R.; Villarreal, M. A. Vinardo: A Scoring Function Based on Autodock Vina Improves Scoring, Docking, and Virtual Screening. *PLoS One* **2016**, *11*, No. e0155183.

(36) Trott, O.; Olson, A. J. AutoDock Vina: Improving the speed and accuracy of docking with a new scoring function, efficient optimization, and multithreading. *J. Comput. Chem.* **2010**, *31*, 455−461.

(37) McNutt, A. T.; et al. GNINA 1.0: molecular docking with deep learning. *J. Cheminf.* **2021**, *13*, 43.

(38) Pracht, P.; et al. CREST-A program for the exploration of low-energy molecular chemical space. *J. Chem. Phys.* **2024**, *160*, 114110.

(39) Bannwarth, C.; Ehlert, S.; Grimme, S. GFN2-xTB—An Accurate and Broadly Parametrized Self-Consistent Tight-Binding Quantum Chemical Method with Multipole Electrostatics and Density-Dependent Dispersion Contributions. *J. Chem. Theory Comput.* **2019**, *15*, 1652−1671.

(40) Schmidt, M. W.; et al. General atomic and molecular electronic structure system. *J. Comput. Chem.* **1993**, *14*, 1347−1363.

(41) Summa, C. M.; Langford, D. P.; Dinshaw, S. H.; Webb, J.; Rick, S. W. Calculations of Absolute Free Energies, Enthalpies, and Entropies for Drug Binding. *J. Chem. Theory Comput.* **2024**, *20*, 2812−2819.

(42) Linkuvienė, V.; et al. Thermodynamic, kinetic, and structural parameterization of human carbonic anhydrase interactions toward enhanced inhibitor design. *Q. Rev. Biophys.* **2018**, *51*, No. e10.

(43) Baronas, D.; et al. Inhibitor binding to metal-substituted metalloenzyme: Sulfonamide affinity for carbonic anhydrase IX. *J. Inorg. Biochem.* **2024**, *256*, No. 112547.

https://doi.org/10.1021/acs.jmedchem.5c01421
J. Med. Chem. 2025, 68, 17752−17773

(44) Jackman, G. B.; Petrow, V.; Stephenson, O.; Wild, A. M. Studies in the Field of Diuretic Agents. Part VI Some Sulphamoylbenzoic Acids. *J. Pharm. Pharmacol.* **1962**, *14*, 679−686.
(45) Jackman, G. B.; Petrow, V.; Stephenson, O.; Wild, A. M. Studies in the Field of Diuretic Agents. *J. Pharm. Pharmacol.* **1963**, *15*, 202−211.
(46) Englert, H. C.; Lang, H.-J.; Linz, W.; Schoelkens, B.; Scholz, W. *Benzoylguanidines, a Process for Their Preparation, Their Use as Medicaments and Medicaments Containing Them*; 1992.
(47) Mickevičiūtė, A.et al.Recombinant Production of 12 Catalytically Active Human CA Isoforms. In *Carbonic Anhydrase as Drug Target: Thermodynamics and Structure of Inhibitor Binding*; Matulis, D., Ed.; Springer International Publishing: Cham, 2019; pp 15−37.
(48) Leitans, J.; et al. Efficient Expression and Crystallization System of Cancer-Associated Carbonic Anhydrase Isoform IX. *J. Med. Chem.* **2015**, *58*, 9004−9009.
(49) Grüner, B.; et al. Metallacarborane Sulfamides: Unconventional, Specific, and Highly Selective Inhibitors of Carbonic Anhydrase IX. *J. Med. Chem.* **2019**, *62*, 9560−9575.
(50) Kazlauskas, E.; Petrauskas, V.; Paketurytė, V.; Matulis, D. Standard operating procedure for fluorescent thermal shift assay (FTSA) for determination of protein−ligand binding and protein stability. *Eur. Biophys. J.* **2021**, *50*, 373−379.
(51) Gedgaudas, M.; Baronas, D.; Kazlauskas, E.; Petrauskas, V.; Matulis, D. Thermott: A comprehensive online tool for protein−ligand binding constant determination. *Drug Discovery Today* **2022**, *27*, 2076−2079.
(52) Lingė, D.; et al. PLBD: protein−ligand binding database of thermodynamic and kinetic intrinsic parameters. *Database* **2023**, *2023*, baad040.
(53) Khalifah, R. G. The carbon dioxide hydration activity of carbonic anhydrase. I. Stop-flow kinetic studies on the native human isoenzymes B and C. *J. Biol. Chem.* **1971**, *246*, 2561−2573.
(54) Williams, J. W.; Morrison, J. F. The kinetics of reversible tight-binding inhibition. In *Methods in Enzymology*; Academic Press: 1979; Vol. *63*, pp 437−467.
(55) Cheng, Y.-C.; Prusoff, W. H. Relationship between the inhibition constant (Ki) and the concentration of inhibitor which causes 50% inhibition (I50) of an enzymatic reaction. *Biochem. Pharmacol.* **1973**, *22*, 3099−3108.
(56) Snyder, P. W.; et al. Mechanism of the hydrophobic effect in the biomolecular recognition of arylsulfonamides by carbonic anhydrase. *Proc. Natl. Acad. Sci. U. S. A.* **2011**, *108*, 17889−17894.
(57) Emsley, P.; Cowtan, K. Coot: model-building tools for molecular graphics. *Acta Crystallogr. Biol. Crystallogr.* **2004**, *60*, 2126−2132.
(58) Kabsch, W. XDS. *Acta Crystallogr. Sect. D* **2010**, *D66*, 125−132.
(59) Battye, T. G. G.; Kontogiannis, L.; Johnson, O.; Powell, H. R.; Leslie, A. G. W. iMOSFLM: a new graphical interface for diffraction-image processing with MOSFLM. *Acta Crystallogr. D Biol. Crystallogr.* **2011**, *67*, 271−281.
(60) Leslie, A. G. W. The integration of macromolecular diffraction data. *Acta Crystallogr. Biol. Crystallogr.* **2006**, *62*, 48−57.
(61) Evans, P. Scaling and assessment of data quality. *Acta Crystallogr. D Biol. Crystallogr.* **2006**, *62*, 72−82.
(62) Vagin, A.; Teplyakov, A. MOLREP: an Automated Program for Molecular Replacement. *J. Appl. Crystallogr.* **1997**, *30*, 1022−1025.
(63) Leitans, J.; et al. Structural Basis of Saccharin Derivative Inhibition of Carbonic Anhydrase IX. *ChemMedChem* **2023**, *18*, No. e202300454.
(64) Murshudov, G. N.; Vagin, A. A.; Dodson, E. J. Refinement of macromolecular structures by the maximum-likelihood method. *Acta Crystallogr. Biol. Crystallogr.* **1997**, *53*, 240−255.
(65) Hanwell, M. D.; et al. Avogadro: An advanced semantic chemical editor, visualization, and analysis platform. *J. Cheminf.* **2012**, *4*, 17.
(66) Vagin, A. A.; et al. REFMAC5 dictionary: organization of prior chemical knowledge and guidelines for its use. *Acta Crystallogr. Biol. Crystallogr.* **2004**, *60*, 2184−2195.
(67) Lebedev, A. A.; et al. JLigand: a graphical tool for the CCP4 template-restraint library. *Acta Crystallogr. D Biol. Crystallogr.* **2012**, *68*, 431−440.
(68) Meng, E. C.; et al. UCSF ChimeraX: Tools for structure building and analysis. *Protein Sci.* **2023**, *32*, No. e4792.
(69) Pettersen, E. F.; et al. UCSF ChimeraX: Structure visualization for researchers, educators, and developers. *Protein Sci. Publ. Protein Soc.* **2021**, *30*, 70−82.
(70) Goddard, T. D.; et al. UCSF ChimeraX: Meeting modern challenges in visualization and analysis. *Protein Sci. Publ. Protein Soc.* **2018**, *27*, 14−25.
(71) Halgren, T. A. Merck molecular force field. I. Basis, form, scope, parameterization, and performance of MMFF94. *J. Comput. Chem.* **1996**, *17*, 490−519.
(72) Halgren, T. A. Merck molecular force field. II. MMFF94 van der Waals and electrostatic parameters for intermolecular interactions. *J. Comput. Chem.* **1996**, *17*, 520−552.
(73) Halgren, T. A. Merck molecular force field. III. Molecular geometries and vibrational frequencies for MMFF94. *J. Comput. Chem.* **1996**, *17*, 553−586.
(74) Halgren, T. A.; Nachbar, R. B. Merck molecular force field. IV. conformational energies and geometries for MMFF94. *J. Comput. Chem.* **1996**, *17*, 587−615.
(75) Halgren, T. A. Merck molecular force field. V. Extension of MMFF94 using experimental data, additional computational data, and empirical rules. *J. Comput. Chem.* **1996**, *17*, 616−641.
(76) Halgren, T. A. MMFF VI. MMFF94s option for energy minimization studies. *J. Comput. Chem.* **1999**, *20*, 720−729.
(77) O'Boyle, N. M.; et al. Open Babel: An open chemical toolbox. *J. Cheminf.* **2011**, *3*, 33.
(78) Bell, E. W.; Zhang, Y. DockRMSD: an open-source tool for atom mapping and RMSD calculation of symmetric molecules through graph isomorphism. *J. Cheminf.* **2019**, *11*, 40.
(79) Chai, J.-D.; Head-Gordon, M. Long-range corrected hybrid density functionals with damped atom−atom dispersion corrections. *Phys. Chem. Chem. Phys.* **2008**, *10*, 6615−6620.
(80) Dunning, T. H. Gaussian basis sets for use in correlated molecular calculations. I. The atoms boron through neon and hydrogen. *J. Chem. Phys.* **1989**, *90*, 1007−1023.
(81) Woon, D. E.; Dunning, T. H., Jr. Gaussian basis sets for use in correlated molecular calculations. III. The atoms aluminum through argon. *J. Chem. Phys.* **1993**, *98*, 1358−1371.
(82) Barone, V.; Cossi, M. Quantum Calculation of Molecular Energies and Energy Gradients in Solution by a Conductor Solvent Model. *J. Phys. Chem. A* **1998**, *102*, 1995−2001.
(83) Bannwarth, C.; et al. Extended tight-binding quantum chemistry methods. *Wiley Interdiscip. Rev.: Comput. Mol. Sci.* **2021**, *11*, No. e1493.
(84) Ehlert, S.; Stahn, M.; Spicher, S.; Grimme, S. Robust and Efficient Implicit Solvation Model for Fast Semiempirical Methods. *J. Chem. Theory Comput.* **2021**, *17*, 4250−4261.

https://doi.org/10.1021/acs.jmedchem.5c01421
J. Med. Chem. 2025, 68, 17752−17773